GEOPHYSICS

Original article
EDN: OTFBNN
DOI: 10.21285/2686-9993-2025-48-2-160-184

Palaeomagnetic correlation of Tunguska syneclise traps of Siberian platform with Permian-Triassic global stratotype of Zhejiang Province, Southern China

Konstantin M. Konstantinov[a]✉, Mikhail D. Tomshin[b], Innokentiy K. Konstantinov[c], Anatolii N. Popov[d], Veniamin E. Pozdniakov[e], Shen Yi[f], Ziton Zhou[g]

[a,c–e]*Irkutsk National Research Technical University, Irkutsk, Russia*
[b]*Diamond and Precious Metal Geology Institute, Siberian Branch of the Russian Academy of Sciences, Yakutsk, Russia*
[f,g]*Nanjing University, Nanjing, China*

Abstract. The purpose of the International Chinese-Russian Geological Expedition of students and teachers in Nanjing and the Yangtze River Delta (China) from October 26 to November 9, 2024 was to establish common connections and patterns in the geological structure and development of the Siberian and South China platforms. The group visited a number of sites of high scientific importance in order to understand the formation patterns of the modern appearance of East Asia beginning from the Late Permian-Early Triassic period (about 250 million years ago). Based on palaeomagnetic data, it was revealed that at the Permian-Triassic boundary these lithospheric blocks were located more than 1,500 km apart separated by the Mongol-Okhotsk Ocean, which closed at the end of the Early Cretaceous period (about 125 million years ago). That was the time when Siberian platform featured active tectonic and magmatic processes related to the Tunguska syneclise trap formation while calm sedimentation of terrigenous-sedimentary strata in marine conditions took place on the South China platform. These geological processes have become the main objects of the research presented in the article. The methodology consisted of collecting and analyzing quantitative data indicating the synchronicity of specified events in time, which will find application in solving a wide range of geological problems including interregional correlations of stratigraphic sections, tectonic-magmatic processes, study of catastrophic phenomena, etc. Materials from paleontological, isotopic, paleomagnetic and other studies (authors' and published by other researchers) were used as a factual basis. The conducted research has shown that the deposition time of the Katangsky volcanic complex basites of the Tunguska syneclise corresponds to the Permian-Triassic boundary of the Meishan section D (Changxing District, Zhejiang Province, South China).

Keywords: Siberian platform, South China platform, Tunguska syneclise, Permian period, Triassic period, trap magmatism, palaeomagnetic reconstructions

Funding: The research was conducted within the framework of the cooperation program between the students of Irkutsk National Research Technical University (Russia) and Nanjing University (China) "Baikal – the pearl of the World".

Acknowledgements: The authors would like to express their deep gratitude to the staff of the Siberian School of Geosciences Institute of Irkutsk National Research Technical University: Candidate of Geological and Mineralogical Sciences L.I. Auzina, Scientific Director of the Institute, Candidate of Geological and Mineralogical Sciences A.V. Parshin, Head of the Department of Domestic and Foreign Communications S.A. Khristova, as well as Professor Yongzhan Zhang of Nanjing University for their great assistance provided in conducting international geological expeditions to the lake Baikal and the Yangtze River Delta.

For citation: Konstantinov K.M., Tomshin M.D., Konstantinov I.K., Popov A.N., Pozdniakov V.E., Yi Sh., et al. Palaeomagnetic correlation of Tunguska syneclise traps of Siberian platform with Permian-Triassic global stratotype of Zhejiang Province, Southern China. *Earth sciences and subsoil use.* 2025;48(2):160-184. https://doi.org/10.21285/2686-9993-2025-48-2-160-184. EDN: OTFBNN.

© Konstantinov K.M., Tomshin M.D., Konstantinov I.K., Popov A.N., Pozdniakov V.E., Yi Sh., Zhou Z., 2025

ГЕОФИЗИКА

Научная статья
УДК 550.838.5

Палеомагнитная корреляция траппов Тунгусской синеклизы Сибирской платформы с глобальным стратотипом пермо-триаса провинции Чжэцзян Южного Китая

К.М. Константинов[a]✉, М.Д. Томшин[b], И.К. Константинов[c], А.Н. Попов[d], В.Е. Поздняков[e], Ш. И[f], Ц. Чжоу[g]

[a,c–e]*Иркутский национальный исследовательский технический университет, Иркутск, Россия*
[b]*Институт геологии алмаза и благородных металлов СО РАН, Якутск, Россия*
[f,g]*Нанкинский университет, Нанкин, Китай*

Резюме. Целью проведения Международной китайско-российской геологической экспедиции в г. Нанкине и дельте реки Янцзы (Китай) в период с 26 октября по 9 ноября 2024 г., состоящей из студентов и преподавателей, являлось установление общих связей и закономерностей в геологическом строении и развитии Сибирской и Южно-Китайской платформ. Группа посетила ряд объектов, имеющих высокое научное значение для понимания формирования современного облика Восточной Азии, начиная с позднепермского-раннетриасового периода (около 250 млн лет). На основе палеомагнитных данных было выявлено, что на границе перми – триаса указанные литосферные блоки были удалены друг от друга на более чем 1500 км. В это время между ними существовал Монголо-Охотский океан, который закрылся в конце раннего мелового периода (около 125 млн лет). В то время на Сибирской платформе протекали активные тектоно-магматические процессы, связанные с формированием траппов Тунгусской синеклизы, а на Южно-Китайской платформе проходило спокойное осадконакопление терригенно-осадочных толщ в морских условиях. Именно эти геологические процессы стали основными объектами представленного в статье исследования. Методика состояла в сборе и анализе количественных данных, свидетельствующих о синхронности указанных событий во времени, которые найдут применение в решении широкого круга таких геологических задач, как межрегиональные корреляции стратиграфических разрезов, тектоно-магматических процессов, изучение катастрофических явлений и др. В качестве фактографической основы были использованы материалы по палеонтологическим, изотопным, палеомагнитным и другим исследованиям (собственные и опубликованные другими авторами). Благодаря проведенному исследованию было показано, что время внедрения базитов катангского вулканического комплекса Тунгусской синеклизы корреспондируется с пермо-триасовой границей разреза Мейшань D (округ Чансин, провинция Чжэцзян, Южный Китай).

Ключевые слова: Сибирская платформа, Южно-Китайская платформа, Тунгусская синеклиза, пермский период, триасовый период, трапповый магматизм, палеомагнитные реконструкции

Финансирование: Исследования проведены в рамках программы сотрудничества студентов Иркутского национального исследовательского технического университета (Россия) и Нанкинского университета (Китай) «Байкал – жемчужина Мира».

Благодарности: Авторы выражают огромную благодарность сотрудникам института «Сибирская школа геонаук» Иркутского национального исследовательского технического университета: кандидату геолого-минералогических наук Л.И. Аузиной, научному руководителю института кандидату геолого-минералогических наук А.В. Паршину, руководителю отдела внутренних и внешних коммуникаций С.А. Христовой, а также профессору Нанкинского университета Юнчжань Чжану за огромную помощь, оказанную в проведении международных геологических экспедиций на оз. Байкал и в дельте р. Янцзы.

Для цитирования: Константинов К.М., Томшин М.Д., Константинов И.К., Попов А.Н., Поздняков В.Е., И Ш. [и др.]. Палеомагнитная корреляция траппов Тунгусской синеклизы Сибирской платформы с глобальным стратотипом пермо-триаса провинции Чжэцзян Южного Китая // Науки о Земле и недропользование. 2025. Т. 48. № 2. С. 160–184. https://doi.org/10.21285/2686-9993-2025-48-2-160-184. EDN: OTFBNN.

Introduction

At the Permian-Triassic boundary in the Siberian Platform, a unique outpouring of basites (basalts, dolerites, tuffs, etc.) occurred on a unique scale. These rocks of basic composition, called Siberian traps, are now developed mainly within the Tunguska syneclise [1–6]. The total thickness of lavas and tuffs here reaches 3000 m in some places. Intrusive traps are predominantly distributed in the eastern part of the platform in the territory of the Republic of Yakutia, which are represented by extended fields of sills and rare dykes marking zones of large crustal rifts on the eastern margin of the Tunguska syneclise, on the southwestern and northeastern slopes of the Anabarsky anteclise.

Magmatism began with the introduction of sills and dykes, then intrusive-effusive activity

with the outpouring of a huge volume of lavas, formation of eruptive apparatuses and accumulation of tuffogenic-sedimentary strata becomes the leading one [6, 7]. On the eastern margin of the Tunguska syneclise, tiered hypabyssal sills are formed, extending eastwards for many tens and even hundreds of kilometres from the magma-supplying zones. Near the latter, the thickness of sills reaches 500 m with its gradual decrease to 10–15 m at the frontal parts of deposits. Dikes usually represent magma-supply channels and are generally few in number. Multilayered sills with a total thickness of several hundred metres were discovered by drilling along the sides of the syneclise in the Paleozoic cover.

The concept of the Siberian traps province includes the area of distribution of close in age magmatic rocks of different composition – from ultrabasic rocks, for example (meimechites), to acidic rocks (rhyolites and granites) [4, 6–10]. Tholeiitic basalts prevail among traps, petrochemical and geochemical features of which are determined by the processes of initial magma formation. Compared to basites of rift zones, they are characterised by reduced and usual for tholeiites contents of TiO_2, P_2O_5 and high concentrations of Ni and Cg. They are steadily depleted in V, Sr, Ba and B.

The age of trap magmatism of the Siberian Platform, according to geological data, is usually determined as late Permian-early Triassic. K-Ag dating (hundreds of determinations) gives a wide range of values: from 270 to 220 Ma, i. e. from the beginning of the Permian to almost the end of the Triassic. A special geochronological study of traps in the Norilsk region with dating of zircons and study of their paleomagnetism leads to the conclusion that trap magmatism is confined to the Permian-Triassic boundary and lasted less than 1 Ma (almost instantaneous in the geological time scale) [11]. This type of magmatism is best explained by a mantle jet (plume) [7, 12, 13]. According to the data, the Siberian Platform in the late Permian-early Triassic (about 250 Ma) was located in the northern polar region and passed over the Icelandic hot spot (Fig. 1).

The eruption of the Siberian traps was one of the largest terrestrial volcanic eruptions in the Phanerozoic history of the Earth. The total volume of volcanic material is estimated at 2×10^6–3×10^6 km^3 [11, 14]. As a result of volcanism, which occurred in an exceptionally short time, the $S0_2$ and volcanic dust (the ash) content in the Earth's atmosphere increased dramatically, leading to acid rain and global climate cooling. The Permian-Triassic boundary in Earth's history is notable for the extinction of many groups of organisms and abrupt changes in global sea level (up to 280 m), which include two periods of abrupt sea regression and two periods of more intense transgression over several million years. These changes are attributed to rapid climate fluctuations due to the increase in polar ice and its subsequent melting.

Active tectono-magmatic operation has determined the metallogeny of the Siberian traps, with which deposits of copper, iron, platinum and other minerals and building materials can be associated.

In this regard, the study of the Siberian traps is of high scientific and applied importance. One of the priority issues is to establish the sequence of formation of basites, which determines the relevance of their comprehensive study. Despite the fact that extensive literature has been devoted to the solution of this question, this problem is still debatable.

Thus, the purpose of our research is to select a basite reference object, relative to which regional correlations of traps of the Tunguska syneclise, Norilsk region, Molodo-Popigai fault zone and other tectono-magmatic structures of Western and Eastern Siberia can be made. The main condition for determining such a reference point should be its reliable connection with the global stratotype[1]. One of the nearest such objects is the Permian-Triassic terrigenous-sedimentary rock sections in southern China[2] [17].

According to the palaeogeographic reconstruction (see Fig. 1), in the Early Triassic (approximately 250 Ma), the Siberian, North and South China Platforms were located in the northern hemisphere, but were separated by the Mongolian-Okhotsk palaeoocean [15, 16]. At this time, the Siberian Platform

[1] Global Stratotype Section and Point (GSSP – Global Stratotype Section and Point) or "Golden Nail" is an internationally agreed reference point on the stratigraphic section, which defines the lower boundary of the stage on the geochronological scale. The work of defining the GSSP is carried out by the International Commission on Stratigraphy (ICS), part of the International Union of Geological Sciences. Many, but not all, global stratotypes are based on palaeontological variations. For this reason, GSSPs are usually described by reference to transitions between different faunal stages, although many more faunal stages have been described than global stratotypes. Work on defining GSSPs began in 1977. As of 2024, 79 of the 101 tiers that require global stratotypes have a ratified GSSP.

[2] Murphy M.A., Salvador A. (eds). *International stratigraphic guide: an abridged version.* Moscow: GEOS; 2002, 38 p. (In Russ.) / Международный стратиграфический справочник: сокращенная версия / отв. ред. Ю.Б. Гладенков. М.: ГЕОС, 2002. 38 с.

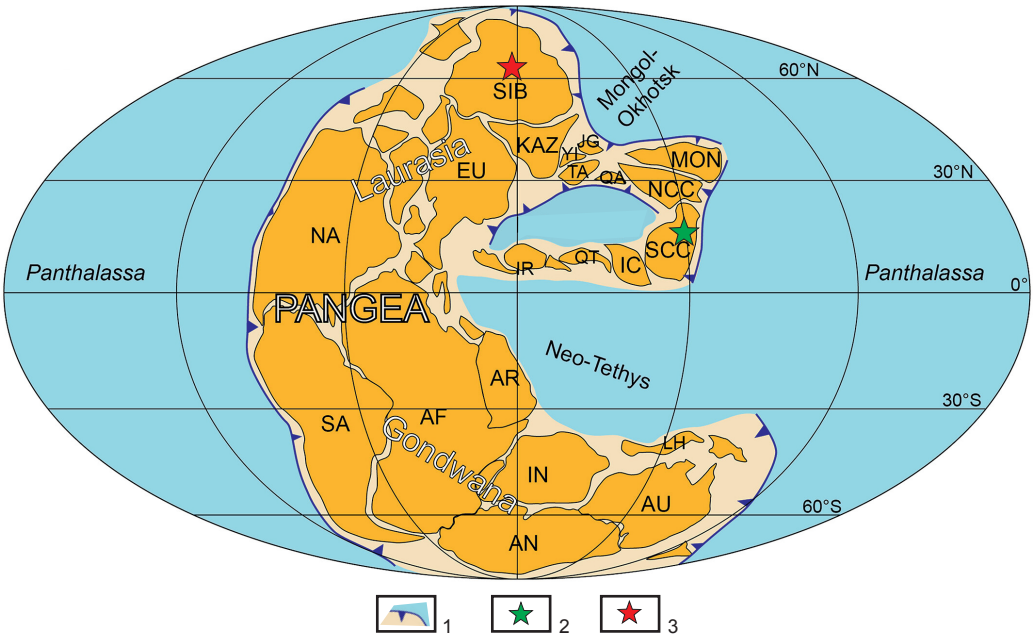

Fig. 1. Paleogeographic reconstruction of the Pangaea supercontinent emphasizing the relative position of main blocks in Eastern Asia in the Early Triassic based on palaeomagnetic data [15, 16]:
1 – subduction boundaries; 2, 3 – localization of the studied objects: 2 – Meishan Province, China, 3 – Western Yakutia, Russia
Abbreviations for blocks (using present-day boundaries):
EU – European craton; KAZ – Kazakhstan block; NA – North America; SA – South America; AF – Africa; IN – India; AN – Antarctic; AU – Australia; AR – Arabian block; IR – Iranian block; QT – Qiangtang block; IC – Indo-Chinese block; LH – Lhasa block

Рис. 1. Палеогеографическая реконструкция суперконтинента Пангея, подчеркивающая относительное положение основных блоков в Восточной Азии в раннем триасе на основе палеомагнитных данных [15, 16]:
1 – границы субдукции; 2, 3 – положение изученных объектов: 2 – провинция Мейшань, Китай, 3 – Западная Якутия, Россия
Сокращения для блоков (с использованием современных границ):
EU – Европейский кратон; KAZ – Казахстанский блок; NA – Северная Америка; SA – Южная Америка; AF – Африка; IN – Индия; AN – Антарктика; AU – Австралия; AR – Аравийский блок; IR – Иранский блок; QT – Цянтанский блок; IC – Индо-Китайский блок; LH – Лхасский блок

was undergoing active trap outpouring associated with the impact of the Icelandic hot spot, and marine sediments were forming on the South China Platform. Clockwise rotation of the Siberian and South China Platforms relative to the North China Platform in the Mesozoic led to the final closure of the Mongolian-Okhotsk Ocean and Paleo-Tethys at the end of the Early Cretaceous (about 125 Ma).

Taking into account the palaeogeographic separation of the regions at the time of formation of the objects under consideration, the main task is to obtain independent isotopic and palaeomagnetic data on the basites of the Siberian Platform and compare them with the available materials on one of the global stratotypes of the South-China Platform.

Materials and methods

Our studies are based on the materials obtained from the Permo-Triassic basites of the eastern side of the Tunguska syneclise (Fig. 2, *a*) over the last 25 years [18–22 and others]. At present, it is established with a high degree of reliability for the traps:

1. Multistage trap magmatism in time [18, 23]. The scheme adopted by geologists identifies three phases: I – intrusive $\gamma\beta P_3$, II – volcanic-subvolcanic β_0-$\gamma\beta P_3$-T_1 and III – intrusive $\gamma\beta T_1$, which correspond to the Olenek-Velingninsky, Katangsky and Kuzmovsky complexes of trap magmatism. The Permo-Triassic age of the considered phases of basites of the eastern side of the Tunguska syneclise is accepted by geologists conditionally.

At the end of the Permian, multistage trap sills of Phase I (moderately ferruginous-titanic group, $TiO_2 \approx 1{,}5$ gram/tonne) were intruded; their outcrops are preserved at the watershed of the Morkoka and Allara-Delingde Rivers and on the slopes of the Morkoka River valley. Characteristic features of phase I sills are the predominance of

subhorizontal intrusions and their strike-slip stability. Precontact changes in the host rocks are weakly expressed. The structure of sills is rather simple, petrographically they are represented by fine- and medium-grained dolerites, less frequently by gabbro-dolerites.

The most widespread in the area are Phase II (magnesia-limestone group, $TiO_2 \approx 1{,}0$ gram/tonne) basites observed in the near-surface horizons of Middle Paleozoic sediments and in the roof of the carbonate basement (Fig. 2, *b*). The trap sills of the Phase II traps are very unstable along strike, form overhangs and blowouts, often split, and form numerous 'windows'. Cases of detachment and transport of blocks of carbonate rocks and kimberlites (Yubileinaya, Podtrappovaya pipes, etc.) by basite intrusions have been noted. Synchronously with the dolerite sills of the intrusive facies characterised above, rocks of the tuffisite and tuff facies, as well as chert-shaped bodies (rootless volcano facies) were formed. Tuffisites are found on low watersheds and basin-like depressions, and are quite widely developed. They have lithoclastic structure and consist of fragments of basalts and hypobasalts of sharp-angular shape. Their formation is associated with certain thermodynamic processes in the near-surface chambers of the forming sills (near eruptive apparatuses or with subvolcanic sills giving local explosion centres in the roof, which then inject into the host rocks) as a result of the breakthrough of gas-saturated tholeiitic melt into the watered coal-bearing strata of terrigenous Permo-Carboniferous rocks. At the same time, the surrounding terrigenous strata contain carbon-containing substances or water-carbon dioxide fluid, due to which secondary boiling increases manifold. This causes a high-power chemical chain reaction and explosive processes, as these components of coal-bearing sediments significantly enhance the physicochemical reactions of phreatomagmatic brecciation and retrograde boiling. This mechanism of tuffisitisation produces peculiar cryptovolcanic structures – explosive calderas and sometimes open vents – explosion funnels with lapilli and conglobreccias. Stokes occur above intrusions of the second facies or among tuffisites (Teguryuk River). Tuffs (Alakit Formation, P_3-T_1al) differ from tuffisites by the presence of admixture of terrigenous material in their composition. The tuffs are dominated by coarse clastic varieties, with medium- and fine clastic varieties occurring less frequently. Thus, the Katangsky volcanic-subvolcanic complex (the Phase II) could most likely be the source of a wide range of volcanic ashes and chemical compounds released into the atmosphere during its formation. The consequence of this effect can be anoxia (complete depletion of oxygen reserves) of the atmosphere, oceans and, as a consequence, mass extinction of organisms.

The Phase III (ferruginous-titanic group, $TiO_2 \approx 2{,}0$ gram/tonne) manifestation of trap magmatism in the Daldyno-Alakitsky area is associated with the Phase III manifestation of trap magmatism in the Daldyno-Alakitsky area, which is associated with shelf-sectional and stratabound basite bodies of various thickness observed mainly among the Lower Paleozoic carbonates (see Fig. 2, *b*). Near the feeder channels, intrusions often form injected uplifts, rejects of carbonate rocks and kimberlite bodies (Komsomolskaya, Krasnopresnenskaya pipes, etc.), and sometimes break through second-phase bodies. Intrusive bodies are, as a rule, secant to the host rocks, their dip angles to the surface are flattened, they are localised mostly in the east and north-east of the area. In the near-contact zones, the host rocks are metamorphosed.

Feeding channels for sills are dikes, which are distributed throughout the territory, but are mapped only in open carbonate fields (see Fig. 2, *a*). Dike intrusions are reflected on magnetic field maps by both positive linear anomalies and negative anomalies. A number of geological features indicate that the negatively magnetised dikes formed at a later stage. Dyke intrusions are rectilinear in plan or arcuately curved, and lie subvertically. Their thicknesses vary from the first metres to the first tens of metres, their length can reach 50–60 km. The most extended dikes have north-western and meridional strike. Dikes with northeastern and latitudinal orientations are less common and do not exceed 10 km in length. Many dikes are abundant with apophyses formed along the fractures dipping the feeder channel. Apophyses of the dikes in the host rocks are developed in the peripheral space (1–2 km) at different depths, as indicated by aeromagnetic survey and drilling data.

2. Each phase has a strict hypsometric (stratigraphic) confinement (see Fig. 2, *b*), from top to bottom: I – armours watersheds, II – intrudes P_3-C_1 terrigenous-sedimentary sediments, III – intrudes rocks of carbonate Early Paleozoic PZ_1 basement (boundary of $O_{2\text{-}3}$kl and S_1ln formations).

3. Diversity of forms of occurrence (dikes, sills, etc.), variability of mineralogical, chemical and petrographic compositions (differentiation, contamination, etc.) [18, 24].

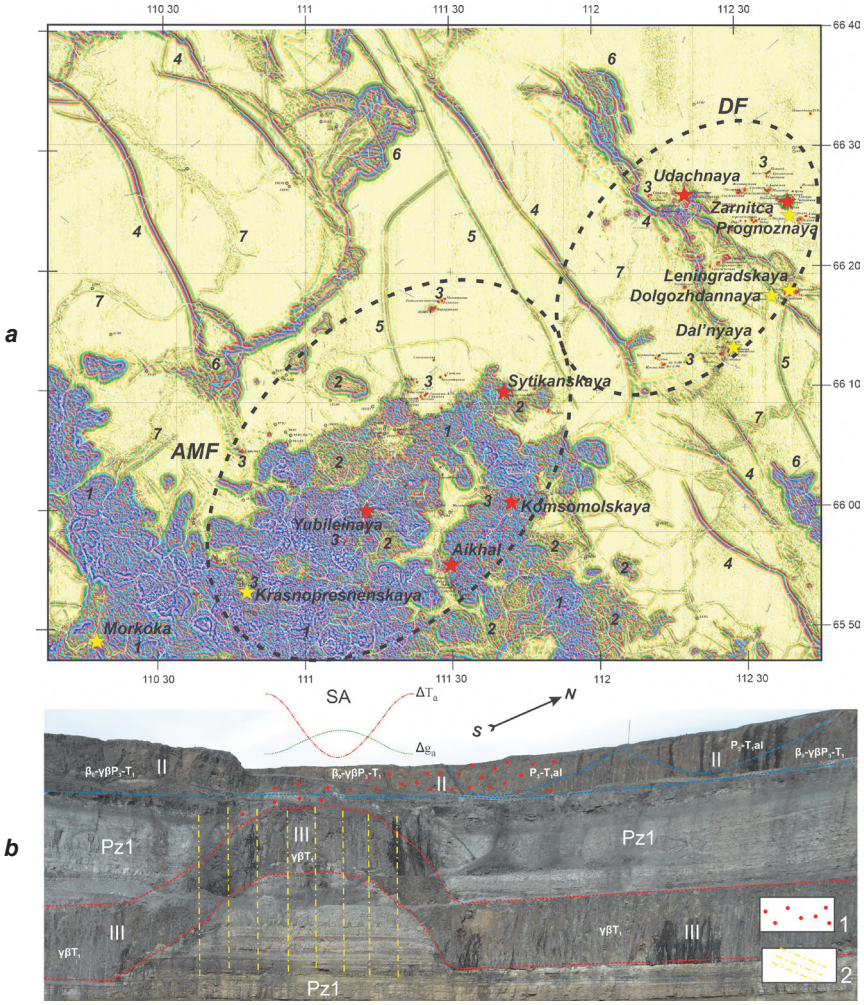

Fig. 2. Trapps of the Daldyn-Alakit diamondiferous region (eastern side of the Tunguska syneclise):
a – position of the studied kimberlite bodies on the summary map of the local component of the magnetic field ΔT_{loc} (red/yellow asterisk – known diamond deposits / off-balance ores)
1–7 – mapping of igneous formations: 1, 2 – sills of trap intrusions reserving watersheds: 1 – Olenek-Velingninsky and Katangsky intrusive complexes (non-separated), 2 – Kuzmovsky intrusive complex; 3 – kimberlite pipes; 4, 5 – dolerite dikes of the Vilyui-Kotui fault zone (supply channels): 4 – positively magnetized, 5 – negatively magnetized; 6 – near-dike crosscutting and substratal dolerite intrusions; 7 – accumulation zones of trap formation destruction products in the floodplains of watercourses;
AMF – Alakit-Markha kimberlite field; DF – Daldyn kimberlite field
b – geological section of the southern northeastern side of the open pit of the Komsomolskaya pipe diamond deposit:
1 – petromagnetic heterogeneities of the firing zone; 2 – zone of increased fracturing;
II, III – basite sills of the second and third introduction phases, respectively
Δg_a – gravity field anomaly; ΔT_a – magnetic field anomaly;
PZ1 – terrigenous-sedimentary rocks of the carbonate basement (Early Paleozoic); SA – structural type anomaly

Рис. 2. Траппы Далдыно-Алакитского алмазоностного района (восточный борт Тунгусской синеклизы):
а – положение изученных кимберлитовых тел на сводной карте локальной составляющей магнитного поля ΔT_{loc} (красная/желтая звездочка – известные месторождения алмазов/забалансовые руды):
1–7 – картирование магматических образований: 1, 2 – силлы трапповых интрузий, бронирующих водоразделы: 1 – оленек-велингнинский и катангский интрузивные комплексы (неразделенные), 2 – кузьмовский интрузивный комплекс; 3 – кимберлитовые трубки; 4, 5 – дайки долеритов Вилюйско-Котуйской зоны разломов (подводящие каналы): 4 – положительно намагниченные, 5 – отрицательно намагниченные; 6 – околодайковые секущие и субпластовые интрузии долеритов; 7 – зоны аккумуляции продуктов разрушения трапповых образований в поймах водотоков
AMF – Алакит-Мархинское кимберлитовое поле; DF – Далдынское кимберлитовое поле
b – геологический разрез южного северо-восточного борта карьера месторождения алмазов трубки Комсомольская:
1 – петромагнитные неоднородности зоны обжига; 2 – зона повышенной трещиноватости;
II, III – силлы базитов, соответственно, второй и третьей фаз внедрения
Δg_a – аномалия гравитационного поля; ΔT_a – аномалия магнитного поля
PZ1 – терригенно-осадочные породы карбонатного цоколя (ранний палеозой);
SA – аномалия структурного типа

4. High-latitude palaeogeographic (see Fig. 1) and present-day positions of the Siberian Platform [25].

5. Inversions of the Earth's magnetic field at the time of the trap introduction [19, 20]: early phases I and II were magnetised by a positive magnetic field, and phase III – by a negative one.

The combination of the last two factors (items 4 and 5), according to the fundamental principle of paleomagnetology of the «central axial dipole» [26], predetermined the characteristic steep positive and negative directions of the vectors of the primary natural remanent magnetisation (NRM, *In*)[3] in the traps 250 Ma ago [19, 20].

We can judge about the time of basite intrusion in the Tunguska syneclise only from the general picture of $^{40}Ar/^{39}Ar$ and U-Pb isotopic dating data (Fig. 3). Against the background of 30 Ma of trap magmatism, the most reliable are two peaks within, respectively: 250±5 and 243±3 Ma. At present, there are only relative correlation schemes of basitic magmatism in separate regions of the Siberian Platform, which dock with each other ambiguously.

Given the complex geological structure of the Tunguska syneclise, in order to unite different tectono-magmatic events into a logical chain, it is necessary to have an age reference, in which the main role was played by precision methods[5] of global importance. These include, first of all, isotopic and palaeomagnetic studies.

The Permian-Triassic boundary, which was approved by IUGS, can serve as the most suitable repartee for correlation of the traps of the Tunguska syneclise; it was defined in Changxing County, Zhejiang Province, South China (Fig. 4) at the base of the Hindeodus *parvus* horizon, at the base of layer 27^{c} of the Meishan D section [17, 44–50]. ICS recognised it as a global stratotype[1] based on the following criteria:

– GSSP must define the lower boundary of the geological stage;

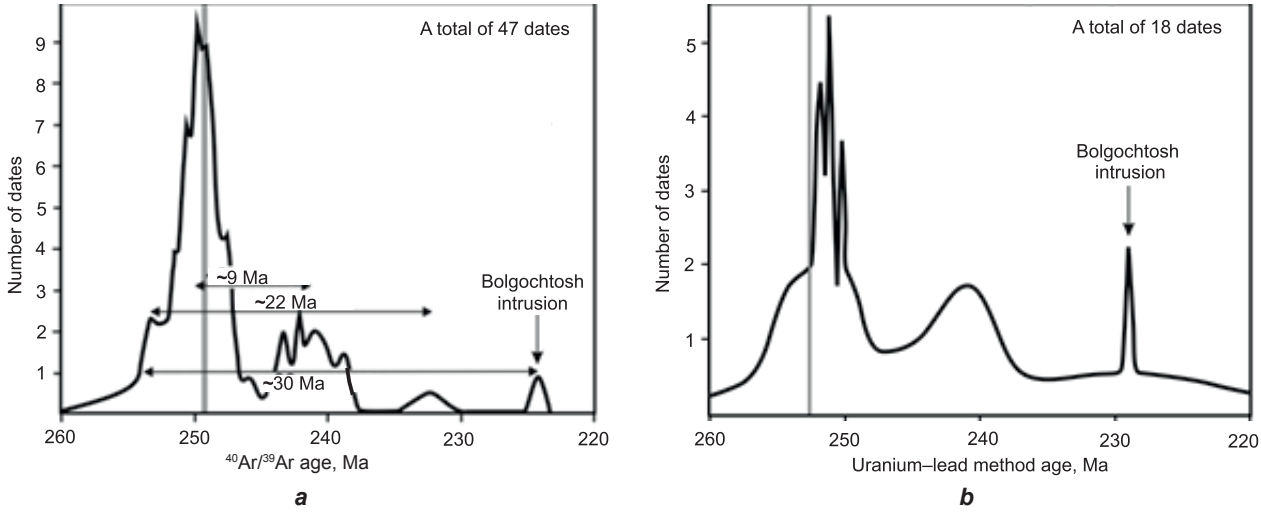

Fig. 3. Age of Siberian traps[4]:
a – distribution histogram of $^{40}Ar/^{39}Ar$ dating (the grey field shows the Permian-Triassic boundary determined by dating sanidines from ashes in the layer 28 of the section D in Meishan Province, China [27–35]); b – dating distribution histogram (uranium–lead method) (the grey field shows the Permian-Triassic boundary determined by dating zircons from ashes in the layer 28 of the section D in Meishan Province, China [14, 36–43])

Рис. 3. Возраст сибирских траппов[4]:
а – гистограмма распределения $^{40}Ar/^{39}Ar$ датировок (серым полем обозначена пермо-триасовая граница, выделенная в результате датирования санидинов из пеплов в слое 28 разреза D в провинции Мейшань в Китае [27–35]); b – гистограмма распределения датировок (уран-свинцовый метод) (серым полем обозначена пермо-триасовая граница, выделенная в результате датирования цирконов из пеплов в слое 28 разреза D в провинции Мейшань в Китае [14, 36–43])

[3] The positive direction of the In vector is downward, the negative direction is upward.
[4] Ivanov A.V. *Intracontinental basaltic magmatism (on the example of mesozoic and cenozoic of Siberia):* dis. … of doctor of geol.-min. sciences. Irkutsk; 2011, 382 p. (In Russ.) / Иванов А.В. Внутриконтинентальный базальтовый магматизм (на примере мезозоя и кайнозоя Сибири): дис. … д-ра геол.-минерал. наук. Иркутск, 2011. 382 с.
[5] Precision method – is a method that allows measurements to be carried out with very high accuracy, i. e. with record low error. It determines the degree of proximity of independent measurement results obtained under specific regulated conditions to each other to an accepted reference value (the reper).

a

b

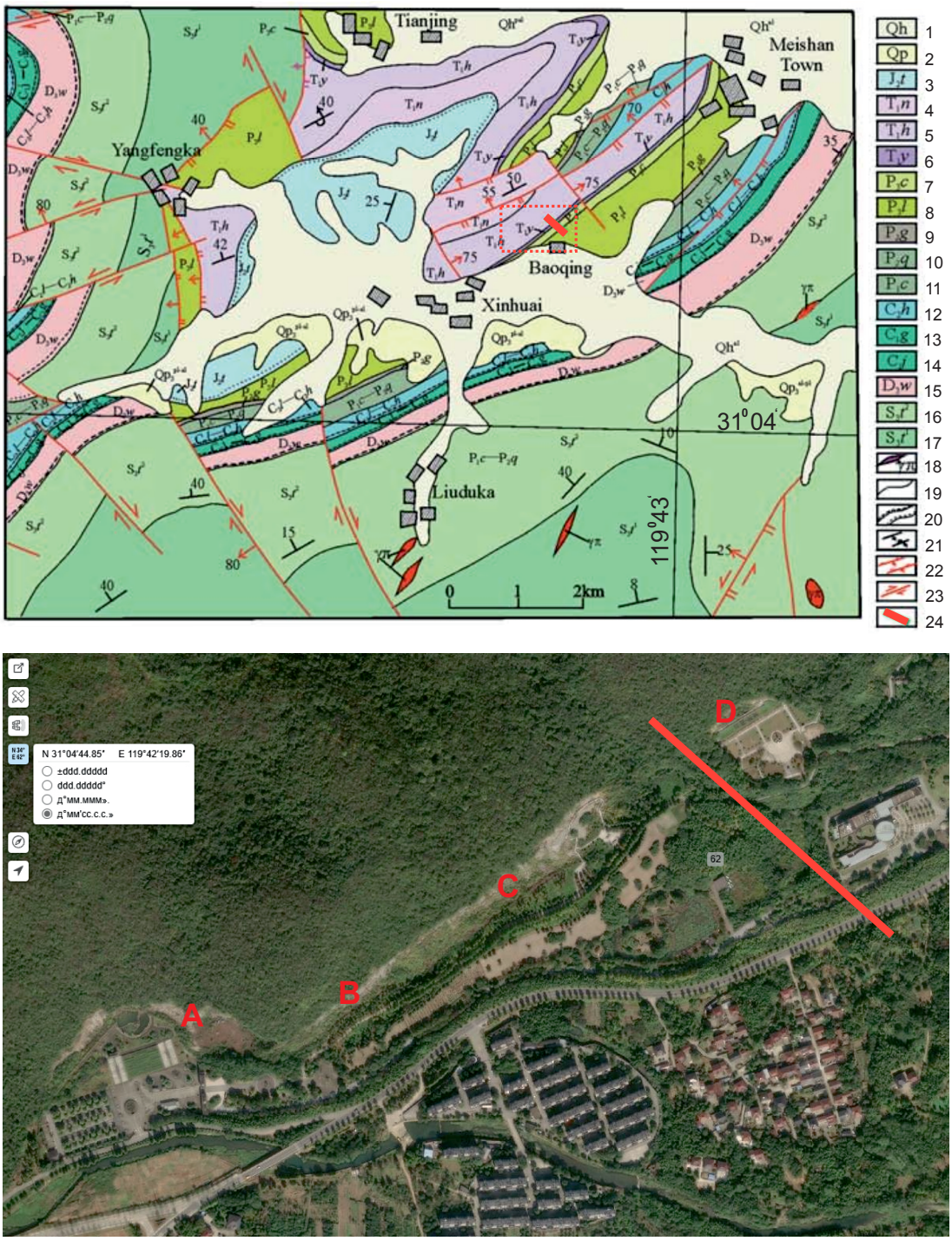

Fig. 4. Geological map [44] and location of the global stratotype park of the Meishan area:
a – geological map: 1 – Holocene; 2 – Pleistocene; 3 – 17 – formations: 3 – Tongshang; 4 – Nanlinghu; 5 – Helongshan; 6 – Yinkeng; 7 – Changxing; 8 – Longtan; 9 – Gufeng; 10 – Qixia; 11 – Chuanshan; 12 – Huanglong; 13 – Gaolishan; 14 – Jinling; 15 – Wutong; 16 – Tangjiawu (Upper mixed bed); 17 – Tangjiawu (Lower mixed bed); 18 – granite-porphyry dike; 19 – conformity boundary; 20 – parallel/angular unconformity boundary; 21 – normal/reverse stratigraphic bedding; 22 – normal/reverse fault; 23 – strike-slip fault; 24 – Meishan, section D
b – park position: A–D – Meishan Geopark quarries (Global Stratotype Section and Point)

Рис. 4. Геологическая карта [44] и положение парка глобального стратотипа района Мейшань:
а – геологическая карта: 1 – голоцен; 2 – плейстоцен; 3 – 17 – свиты: 3 – Туншан; 4 – Наньлинху; 5 – Хелонгшань; 6 – Иньkэн; 7 – Чансин; 8 – Лунтан; 9 – Гуфэн; 10 – Цися; 11 – Чуаньшань; 12 – Хуанлун; 13 – Гаолишань; 14 – Цзиньлин; 15 – Вутун; 16 – Танцзяву (верхний смешанный слой); 17 – Танцзяву (нижний смешанный слой); 18 – гранит-порфировая дайка; 19 – граница соответствия; 20 – параллельная/угловая граница несогласия; 21 – нормальное/обратное стратиграфическое залегание; 22 – нормальный/обратный разлом; 23 – сдвиговый разлом; 24 – Мейшань, разрез D
b – положение парка: A–D – карьеры геопарка Мейшань (Глобальный стратотипический разрез и точка)

– the lower boundary must be defined by a primary marker (usually data on the first occurrence of a fossil species);

– there should also be secondary markers (other fossils, chemical, geomagnetic inversions);

– the horizon in which the marker appears must contain minerals that can be radiometrically dated;

– the marker must have regional and global correlation in outcrops of the same age;

– the marker should be facies independent (without any changes in facies);

– sedimentation must be continuous;

– the outcrop must have sufficient thickness;

– the outcrop should be unaffected by tectonic and sedimentary movements and metamorphism;

– the outcrop must be accessible and readily available for research: it must be quickly accessible (international airport and good roads), well maintained (ideally in a national reserve), in an accessible area, extensive enough to allow repeat sampling, and open to researchers of all nationalities.

The participants of the international expedition visited this stratotypic outcrop (see Fig. 5) and collected important information on it, necessary for global correlation with the Siberian traps. At present, the global Permian-Triassic boundary stratotype is characterised by a wide range of scientific information [17, 44–50].

The Permian-Triassic boundary runs along layer 27, composed of argillic micrites (see Fig. 5, *b*) [45–50]. The main fossils of the Early Triassic sole (layers 27^c and 27^d) are the extinct conodont genus Hindeodus parvus, Ellisonia and Isarcicella isarcica (see Fig. 5, *c, d*). Most likely, the demise of Permian conodonts is due to global anoxia, as indicated by the $\delta^{13}C$ peak of the Protein Data Bank (PDB)[6] plot [51]. This zone has been recorded in 27 localities of 11 provinces of South China, as well as in Selong (Tibet, China), Guryul Gorge (Kashmir), Spiti (India), Abad and Kuh-e-Ali Bashi (Iran), Narmal Nala (Pakistan), Gartner Kofel (Austria), Tesero (Italy), Western America, Arctic regions of Canada, Australia, Timor and other localities [44].

Based on radioisotope studies (Table 1), the age boundary of the Permian and Triassic is estimated to be 252.17±0.06 Ma. The results of recent radioisotopic ages of both U/Pb and $^{40}Ar/^{39}Ar$, according to the dating of volcanic ash, the age of Permian-Triassic boundary in marine strata and the age of mass extinction are indistinguishably 252.5±0.2 Ma [35, 53].

Studies [58–62] have shown that the Meishan C and D sections can be divided into five subzones of normal polarity and four subzones of reversed polarity (Fig. 6). The lower part of the Changxi Stage has normal polarity, and the upper part has both normal and reverse polarity. In general, the Permian-Triassic boundary is characterised, with a high degree of probability, by the direct polarity of the Earth's magnetic field (MS5n).

To solve the problem of regional paleomagnetic correlation of the traps of the Tunguska syneclise of the Siberian Platform with the global stratotypic section of the Permian-Triassic terrigenous-sedimentary formations in the Zhejiang Province of South China (see Fig. 4), we selected basites of three phases of intrusion of the Alakit-Markha kimberlite field (see Fig. 2, *a*). One of the important objects for studying the sequence of basite formation is the Komsomolskaya pipe diamond field, in the quarry of which two sills of dolerites of II and III phases of intrusion are exposed [10, 18] (see Fig. 2, *b*). The dolerite sill of the II phase lies horizontally on the watershed, while the dolerite sill of the III phase is emplaced in the Early Paleozoic carbonate basement. The Phase III sill, rising in the area of increased fracturing to the footwall of the Phase II sill, forms a sigmoid and thereby cuts the northwestern block of the diatreme to form a kimberlite detachment.

Studies of basites of the Tunguska syneclise included:

1. Field work on selection of oriented pieces [26]. In total, more than 600 pieces were sampled;

2. Sample preparation – making 3–4 cubes with 20 mm rib from the samples. In total about 2000 cubes were obtained;

3. Laboratory research of physical properties (density, magnetisation), petro- and paleomagnetic analyses. The investigations were carried out with modern equipment: magnetic susceptibility *æ* meters (KLY-3s and MFK1-FA, AGICO,

[6] Protein Data Bank (PDB) – is a data bank of three-dimensional structures of proteins and nucleic acids. Information obtained by X-ray crystallography or nuclear magnetic resonance (NMR) spectroscopy, and increasingly by cryo-electron microscopy, is entered into the database by biologists and biochemists from all over the world and is available free of charge through the websites of its member organisations (PDBe, PDBj, RCSB). The PDB is one of the most important resources for scientists working in structural biology. Most scientific journals and some research funding foundations, e. g. NIH in the USA, require authors of articles and grantees to have all structural data posted on the PDB. The PDB contains mainly primary data on the structure of biological molecules, while there are hundreds of other data banks categorising primary data or identifying patterns between molecular structure and evolutionary relatedness.

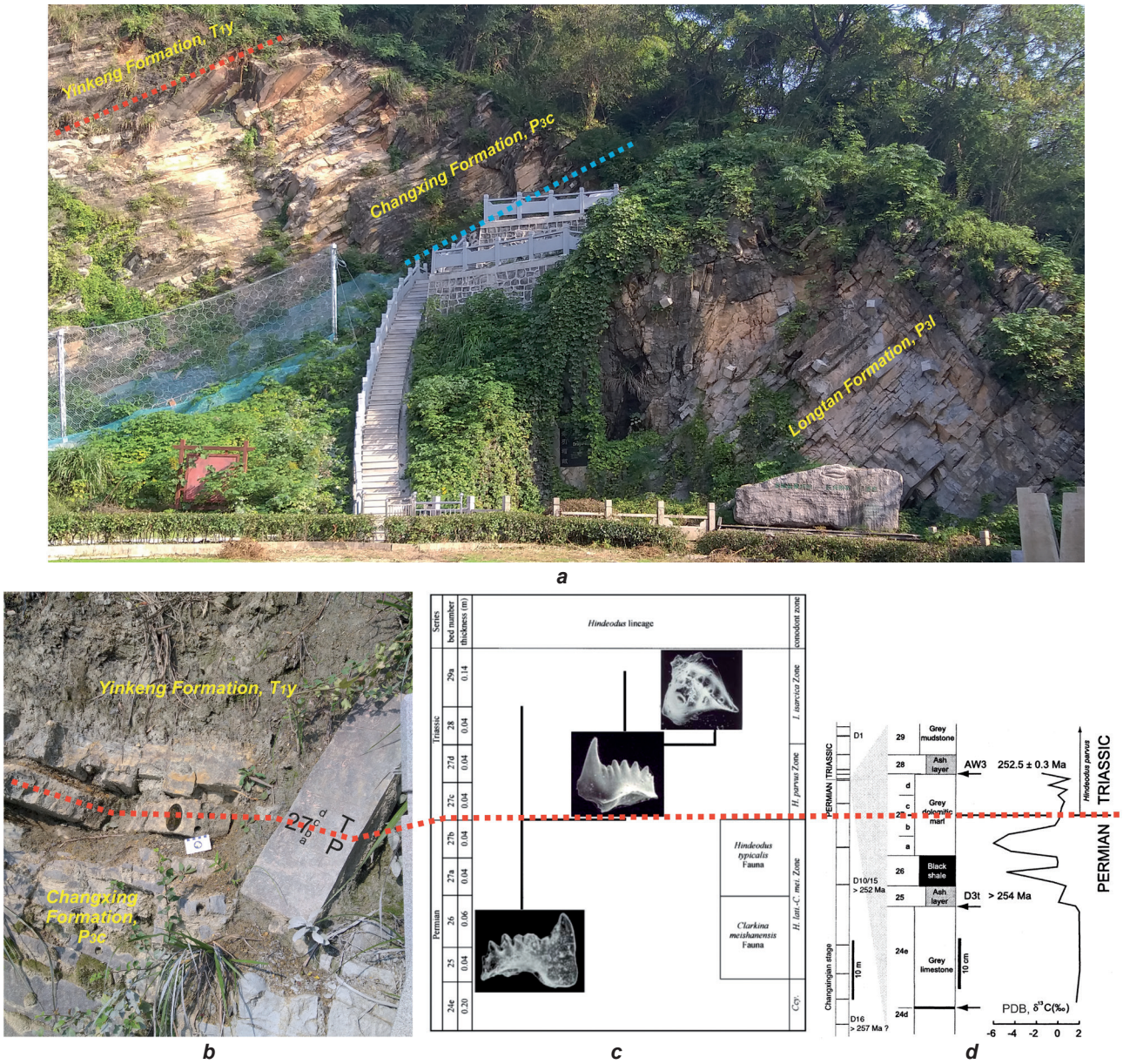

Fig. 5. Meishan D geological section, Changxi County, Zhejiang Province, South China, China [44]:
a – view of Meishan section D with indicated lithostratigraphic units; b – "Golden Nail" (a bronze disc in the middle of the image) or 'type section' of the global boundary stratotype section and the point for the formation of the Permian-Triassic boundary; c – Hindeodus evolutionary lineage at the Permian-Triassic boundary: Ccy – Clarkina changxingensis yini Zone, H. lati. – C. mei. – Hindeodus latidentatus – Clarkina meishanensis; d – detailed stratigraphy for the Permian-Triassic boundary interval at Meishan (South China) with indicated ash layers and assigned ages, three extinction levels (horizontal arrows) and δ^{13}C curve Protein Data Bank [51]. The column to the left shows the stratigraphic sequence exposed at the proposed Permian-Triassic boundary stratotype, section D and section AW, with volcanic ash layers (black bands) and samples collected for isotopic age dating (D16, D10/15, D3t, AW3 and D1) [52]

Рис. 5. Геологический разрез Мейшань D, округ Чансин, провинция Чжэцзян, Южный Китай (Китай) [44]:
a – вид Мейшаньского разреза D с указанием литостратиграфических подразделений; b – «золотой гвоздь» (бронзовый диск в средней части изображения), или типовой разрез глобального пограничного стратотипического разреза и точки для основания пермо-триасового рубежа; c – эволюционная линия Hindeodus на пермо-триасовой границе: Ccy – зона Clarkina changxingensis yini, H. lati. – C. mei. – Hindeodus latidentatus – Clarkina meishanensis; d – подробная стратиграфия для пермо-триасового пограничного интервала в Мэйшане (Южный Китай) с указанием слоев пепла и присвоенного возраста, трех уровней вымирания (горизонтальные стрелки) и δ^{13}C кривая Банка данных о белках [51]. В столбце слева показана стратиграфическая последовательность, обнаженная на предполагаемом пермо-триасовом стратотипе, разрезе D и разрезе AW, со слоями вулканического пепла (черные полосы) и образцами, собранными для датирования изотопного возраста (D16, D10/15, D3t, AW3 и D1) [52]

Table 1. Radiometric dating of the Permian-Triassic boundary at Meishan section
Таблица 1. Радиометрическое датирование границы перми и триаса разреза Мейшань

Bed	References				
	[54]	[55]	[56]	[57]	[52]
36	–	–	250.2±0.2 (U)	252.6±1.2 (S)	–
34	–	–	–	253.6±1.3 (S) 249.2–253.5 (U)	–
33	–	–	250.4±0.5 (U)	–	–
28	–	–	250.7±0.3 (U) –	251.7±1.4 (S) 251.6±0.3 (U)	–
25	251.2±3.4 (S)	249.91±0.15 (Ar)	251.4±0.3 (U)	–	253 (U)
20	–	–	252.3±0.3 (U)	–	–
7	–	–	253.4±0.2 (U)	–	–

Note. S – SHRIMP U/Pb; U – ordinary U/Pb (zircon); Ar – $^{40}Ar/^{39}Ar$.

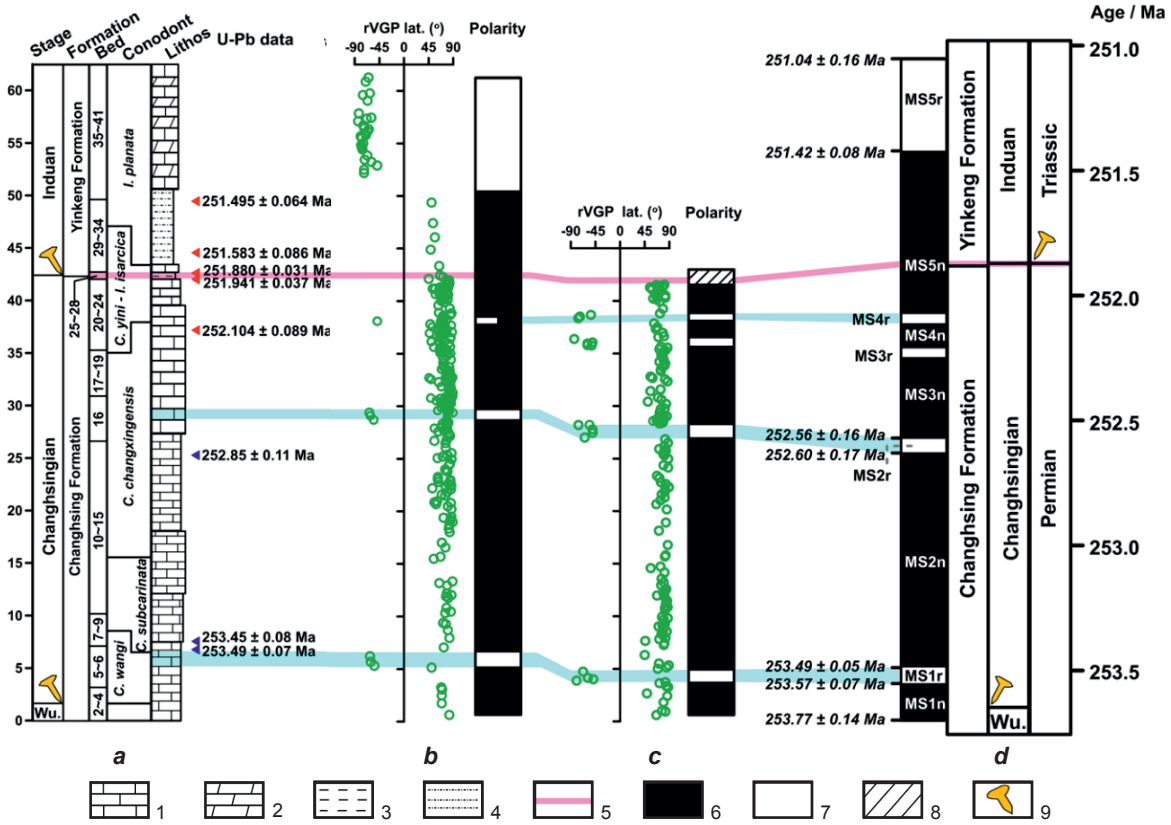

Fig. 6. Magnetostratigraphic results for the Meishan sections (southeastern China) [62]:
a – Meishan section lithology; b – Meishan section C; c – Meishan section D; d – composite magnetozones
Conodont zones are modified from the source [63]. Data (blue and red triangles)
are taken from the sources [64, 65], respectively (uranium-lead method)
rVGP – rotated virtual geomagnetic pole; Wu. – Wuchiapingian; C. – Clarkina; I. – Isarcicella
1 – limenstone; 2 – argillaceous limenstone; 3 – clayey rocks; 4 – mudstone; 5 – maximum interval
of the end-Permian mass extinction; 6 – reverse polarity; 7 – normal polarity; 8 – no data;
9 – "Golden Nail" (Global Stratotype Section and Point)

Рис. 6. Магнитостратиграфические результаты по разрезам Мейшань
(Юго-Восточный Китай) [62]:
a – литология разреза Мейшань; b – Мейшаньский разрез C; c – Мейшаньский разрез D;
d – составленные магнитозоны
Зоны конодонтов модифицированы согласно источнику [63]. Данные (синие и красные треугольники)
взяты из работ [64, 65] соответственно (уран-свинцовый метод)
rVGP – повернутый виртуальный геомагнитный полюс; Wu. – Wuchiapingian; C. – Clarkina; I. – Isarcicella
1 – известняк; 2 – аргиллитовый известняк; 3 – глинистые породы; 4 – аргиллит; 5 – максимальный
интервал конца пермского массового вымирания; 6 – обратная полярность; 7 – нормальная полярность;
8 – нет данных; 9 – «золотой гвоздь» (Глобальный стратотипический разрез и точка)

Czech Republic), spin-magnetometers for measuring NRM vectors (JR-6, AGICO, Czech Republic), demagnetising units with alternating magnetic field (AF-Demagnetizer, Molspin LTD, UK) and temperature (MMTD80, Magnetic Measurements LTD, UK), vibro-magnetometers and magnetic fraction meters (Kazan, KFU, RF), etc.

4. Complex interpretation of geological and geophysical materials.

Results and discussion

The main results of petrophysical, palaeomagnetic and analytical studies of Permo-Triassic basites studied within the eastern side of the Tunguska syneclise (see Fig. 2, *a*) can be summarised as follows:

1. The spectrum of density and magnetic parameters in "natural occurrence" was obtained (Table 2). The values of magnetic parameters of basites have a wide enough range of dispersion. Tuffs and microdolerites have minimum values of magnetisation: $æ \approx 40...50\times10^{-5}$ SI, $In \approx 1...10\times10^{-3}$ A/m, factor $Q \approx 0.05...0.50$ units. The magnetic susceptibility of dolerites of the III phase is relatively higher than that of the I and II phases of embedding, which is determined by the increased iron content [10, 18]. At the same time, the values of NRM vectors and Q factor of phase III basites are relatively lower than those of the early phases of basites. This effect is related to the demagnetising effect of the geomagnetic field on the primary magnetisation of phase III basites.

The *In* vectors, which have both positive and negative directions (see Table 2), regardless of the time of phase introduction (the same phase of basites can be magnetised both positively and negatively), deserve special attention. In terms of the time of formation, the *In* vectors can be both primary (synchronous to the formation of rocks) In^0 and metachronic (secondary, superimposed) In^m. The latter, as a rule, can form different types of petromagnetic inhomogeneities [20]: remagnetisation by the geomagnetic field (type 1), "firing" (type 2); "self-turning" (type 3), thunderstorm strikes (type 4), and "stress" (type 5).

In this connection, it is necessary to establish the palaeomagnetic nature of those and other NRM vectors on the basis of the study of their component composition.

2. Massive palaeomagnetic studies with alternating magnetic field and temperature have shown that the first two phases at the time of their formation were magnetised by the Earth's magnetic field of positive polarity (close to the present-day direction), while phase III was negatively magnetised [20, 21].

This conclusion was confidently proved at the diamond deposit of the Komsomolskaya kimberlite pipe (see Fig. 2, *b*). According to the data of the component paleomagnetic analysis, the sill of phase III basites (Kuzmovsky intrusive complex), rising along the zones of increased fracturing, remagnetises the sill of phase II dolerites (Katangsky volcanic complex) in the endocontact. For example, obr. Kom03-143t5 from the sill of phase III dolerites, after removal of the low-temperature (less than 250 °C) component *A*, has the primary component *B* of the In^0 vector of reversed polarity (Fig. 7, *c*). At the same time, in the overlying dolerites and tuffs of Kom01-24t14 of the II phase, the same component *B* is isolated in the medium-temperature region (from 250 to 450 °C) and is metachronous In^m, while the high-temperature (more than 450 °C) component *D* is primary of direct polarity (Fig. 7, *b*). At a distance from the contact with Phase III, only one primary *D* component is established in the dolerites of the Katangsky complex of the Kom04-236t2 cluster (Fig. 7, *a*). Thus, the paleomagnetic materials (Table 3) clearly indicate a relatively young age of the phase III basites.

Simultaneously, a structural type anomaly is formed above the sigmoidal shape of the sill of phase III associated with its ascent to the footwall of the sill of phase II and remagnetisation of the primary In^0 vectors of the latter in the endocontact from direct to reverse polarity with the formation of In^m (see Fig. 2, *b*) [20, 66]. As a result of firing of dolerites of III phase by sillom, petromagnetic heterogeneity of the second type is formed in the endocontact of basites of II phase. In the process of «temperature» influence, the petromagnetic boundary shifts up the section by 25–30 m relative to the geological (petrodensity boundary). Thus, structural type anomalies are formed on the flanks of such diamond deposits, which are characterised by positive gravity Δg_a (amplitude up to 1.5 mGal) and negative magnetic ΔT_a (amplitude up to -1000 nT) effects. Similar anomalies may reflect diatreme association structures and, therefore, indicate areas promising for the search for kimberlite bodies.

3. $^{40}Ar/^{39}Ar$ geochronological studies of dolerites by the step heating method [67] performed at the V.S. Sobolev Institute of Geology and Mineralogy Siberian Branch of the Russian Academy of Sciences (Novosibirsk) showed that the introduction of sill dolerites of phase II (Katangsky volcanic complex) of the kimberlite pipe diamond deposit of the Komsomolskaya kimberlite pipe corresponds to the Permo-Triassic period and is 255.5±4.3 Ma [66].

Table 2. Magnetic parameter spectrum of Permian-Triassic traps of the eastern side of the Tunguska syneclise
Таблица 2. Спектр магнитных параметров пермо-триасовых траппов восточного борта Тунгусской синеклизы

Site, rock type	*n*	*æ* (*ε*), 10^{-5} SI	*In*				*Q* (*ε*), units
			In (*ε*), 10^{-3} A/m	*Dm*, °	*Jm*, °	*k*, units / α_{95}, °	
First phase (Olenek-Velingninsky complex), $\gamma\beta P_3$							
Morcoca, dolerites	25	1890 (1.03)	5495 (1.07)	150	85	49.1/4.0	6.09 (1.08)
Morcoca, dolerites*	3	1445 (1.06)	4848 (1.06)	100	-80	2036.6/2,7	7.10 (1.01)
Trace, dolerites	130	1765 (1.03)	4100 (1.06)	345	80	10.9/4.0	4.86 (1.06)
Second phase (Katangsky complex), β_0-$\gamma\beta P_3$-T_1							
Aikhal, dolerites	140	1130 (1.03)	2800 (1.05)	80	82	29.4/2.2	5.1 (1.03)
Bistriy, dolerites	95	1490 (1.02)	4550 (1.09)	35	75	4.4/7.9	6.39 (1.09)
Yubileinaya, dolerites	110	1800 (1.02)	4050 (1.03)	35	83	48.9/1.9	4.7 (1.04)
Komsomolskaya, dolerites	130	1300 (1.04)	1700 (1.04)	74	82	38.0/2.1	2.9 (1.05)
Komsomolskaya, dolerites*	60	1155 (1.05)	570 (1.08)	275	-60	13.7/5.2	1.03 (1.07)
Komsomolskaya, tuffs	50	40 (1.04)	10 (1.15)	85	85	15.8/5.3	0.43 (1.14)
Komsomolskaya, tuffs*	55	40 (1.03)	5 (1.14)	290	-60	16.3/5.0	0.42 (1.12)
Alakit, dolerites	45	1600 (1.02)	10445 (1.18)	60	70	3.30/14.3	13.66 (1.17)
Chukuka, dolerites	40	1420 (1.05)	3590 (1.05)	45	85	41.0/3.5	5.30 (1.06)
Cherniy, dolerites	105	1600 (1.02)	5130 (1.06)	55	70	6.3/6.0	6.72 (1.06)
Trace, microdolerites	40	65 (1.01)	5 (1.28)	355	60	6.1/10.1	0.14 (1.27)
Microdoleritoviy dolerites	80	850 (1.05)	1715 (1.07)	50	80	13.5/4.5	4.24 (1.06)
Microdoleritoviy microdolerites	40	65 (1.01)	5 (1.20)	90	85	49.5/3.2	0.15 (1.20)
Sytikanskaya, dolerites*	45	1200 (1.09)	470 (1.11)	320	45	3.7/12.8	0.82 (1.06)
Vodorazdelniy, dolerites	40	1005 (1.12)	3210 (1.15)	65	85	40,9/3,5	6.68 (1.07)
Vodorazdelniy, microdolerites	140	65 (1.01)	1 (1.14)	40	75	4.58/6.5	0.04 (1.12)
Vodorazdelniy, tuffs	55	50 (1.02)	5 (1.09)	95	85	26.0/3.8	0.16 (1.08)
Third phase (Kuzmovsky complex), $\gamma\beta T_1$							
Komsomolskaya, dolerites	180	1500 (1.02)	870 (1.05)	285	-60	11.5/3.3	1.1 (1.05)
Sytikanskaya, dolerites	195	1260 (1.03)	1015 (1.04)	290	-45	6.8/4.2	1.66 (1.07)
Alakit, dolerites	75	1370 (1.09)	1405 (1.11)	300	-60	3.0/11.5	2.15 (1.11)
Bistriy, dolerites	30	2065 (1.02)	1020 (1.07)	330	-10	2.1/24.5	1.03 (1.09)
Chukuka, dolerites	105	1740 (1.02)	1900 (1.13)	345	-40	1.9/14.5	2.28 (1.13)
Sohsolooch, dolerites	50	2070 (1.02)	1020 (1.07)	330	-10	2.1/24.5	1.03 (1.09)
–	1948	–	–	–	–	–	–

Note. n – number of samples participating in the statistics; *In* – absolute values of vectors *In*; *Dm* – mean declination; *Jm* – mean inclination; *k* – heaping; α_{95} – confidence angle with 95 % probability of *In* vectors; the standard multiplier is in parentheses; * – petromagnetic inhomogeneity of type 2 (heating on the sill side of dolerites of third phase).

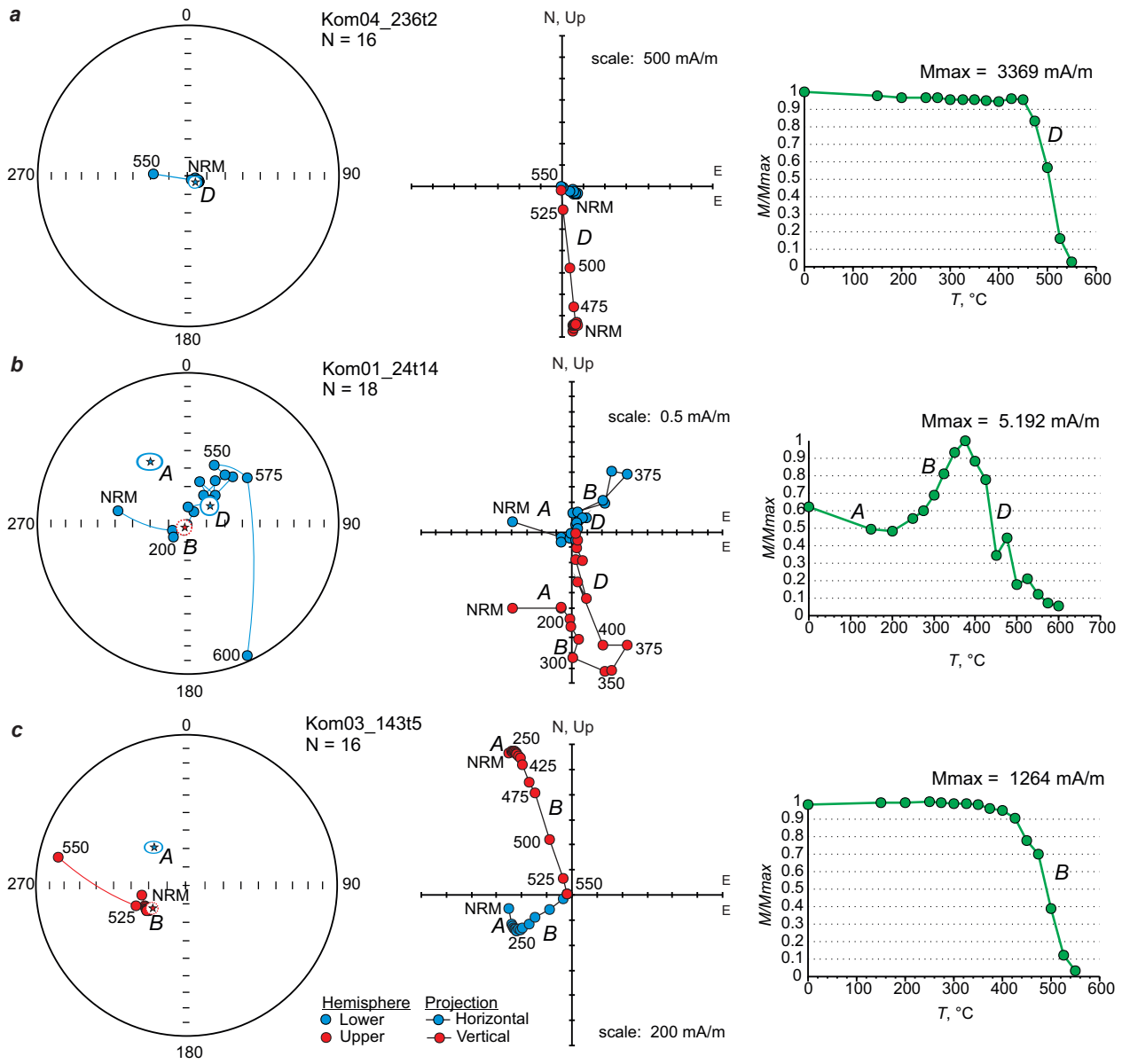

Fig. 7. Paleomagnetic studies of basites of the Katangsky (a, b) and Kuzmovsky (c) volcanic complexes of the Komsomolskaya kimberlite pipe diamond deposit:
a – Katangsky volcanic complex dolerites (phase II); c – Kuzmovsky volcanic complex dolerites (phase III); b – Alakit suite tuffs (see the article for other designations)

Рис. 7. Палеомагнитные исследования базитов катангского (a, b) и кузьмовского (c) вулканических комплексов месторождения алмазов кимберлитовой трубки «Комсомольская»:
a – долериты катангского (II фаза) вулканического комплекса; c – долериты кузьмовского (III фаза) вулканического комплекса; b – туфы алакитской свиты (другие обозначения см. в тексте)

Table 3. Paleomagnetic directions of different-phase basites of the Komsomolskaya kimberlite pipe diamond deposit
Таблица 3. Палеомагнитные направления разнофазных базитов месторождения алмазов кимберлитовой трубки «Комсомольская»

Objects	*n*	*Dm*, °	*Jm*, °	*k*	α_{95}, °
Dolerites, phase III, In^0 (component B)	32	259	-75	12.5	7.5
Dolerites, II phase, In^m (component B)	41	254	-66	9.3	7.7
Tuffs of the Alakit Formation, Phase II, In^m (component B)	11	245	-68	15.9	11.8
Tuffs of the Alakit Formation, Phase II, In^0 (component D)	17	42	80	10.0	11.9
Dolerites, II phase, In^0 (component D)	57	65	82	25.4	3.8

Note. *n* – number of samples; parameters of NRM vectors grouping; *Dm* – mean declination; *Jm* – mean inclination; *k* – heaping; α_{95} – confidence angle with 95 % probability of *In* vectors.

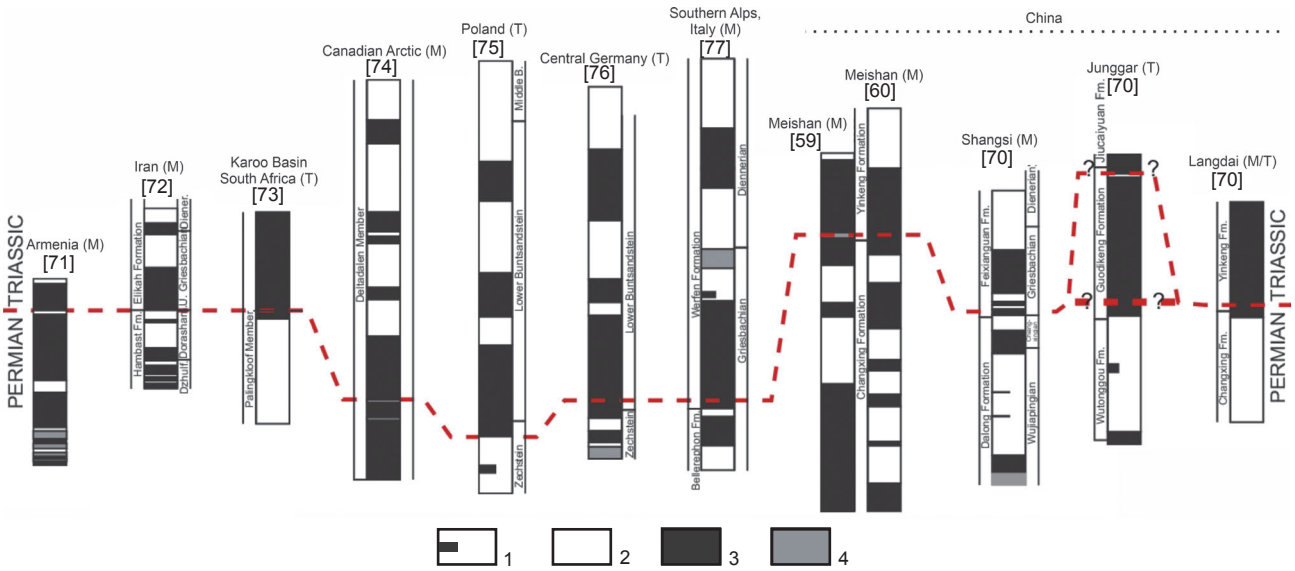

Fig. 8. Correlation of the composite section magnetostratigraphies of the Shangsi, Junggar, and Langdai localities with other Permian-Triassic marine records from around the world [69]:
1 – possible short polarity chron, 2 – reverse polarity, 3 – normal polarity, 4 – no data
T – terrestrial sections; M – marine sections; M/T – paralic[7] sections

Рис. 8. Корреляция магнитостратиграфии составных разрезов из местонахождений Шанси, Чжунгар и Лангдай с другими морскими данными перми – триаса со всего мира [69]:
1 – возможное короткое замыкание хрона; 2 – обратная полярность; 3 – нормальная полярность; 4 – нет данных
T – наземные разрезы; M – морские разрезы; M/T – паралические[7] разрезы

Thus, according to isotopic and palaeomagnetic studies of basites from the eastern side of the Tunguska syneclise, we have for the Katangsky complex (phase II) an age from 259.8 to 251.2 Ma and the direct polarity of the primary magnetisation of In^0 vectors. The data obtained for the Siberian Platform agree well with the geochronological (252.17± 0.06 Ma) and palaeomagnetic (direct polarity) data on Permian-Triassic boundary of the Meishan section of the South China Platform (see Table 1, Fig. 6).

Since the basites of the Kuzmovsky intrusive complex remagnetise the basites of the Katangsky complex, they are relatively younger and, according to [68], may belong to the second stage of magmatic activity of the traps of the Siberian Platform – approximately 244±5 Ma (see Fig. 3).

Fig. 8 shows the magnetostratigraphic correlation of geological sections of the world [69]. The Permian-Triassic boundary is characterised with a high degree of probability by the direct polarity of the Earth's magnetic field [58, 59, 69–78].

Conclusion

In the course of the Sino-Russian geological expedition in Nanjing and the Yangtze River delta, the following results were obtained on the basis of comparison of modern isotopic, paleontological, bio-, chemo- and magnetostratigraphic, etc. data on the Permian-Triassic boundary of the Meishan section of Zhejiang Province, South China Platform (see Fig. 4, 5) with the basites of the eastern side of the Tunguska syneclise of the Siberian Platform (see Fig. 2):

1. The spectrum of values of petrophysical parameters (see Table 2) and palaeomagnetic directions of NRM vectors of basites (see Fig. 7, Table 3).
2. The Katangsky complex may have been a major source of volcanic ash and gases that were transported in the Earth's atmosphere over great distances. Their traces were recorded in the Permian-Triassic Meishan stratotypic section on the South China Platform (see Fig. 5). The abrupt climatic changes associated with its introduction caused the extinction of old organisms and the appearance of new ones (e. g., the conodonts under consideration).
3. The age of basites of the Katangsky volcanic complex (phase II), which corresponds to the Permian-Triassic boundary – approximately 252±2 Ma, was determined. Thus, the basites of this complex can be considered as a Permian-Triassic boundary reper, with which other volcanic complexes of the Tunguska syneclise of the Siberian Platform can be correlated.
4. The age of formation of basites of the Kuzmovsky volcanic complex (phase III) corresponds

[7] A paralitic horizon is a weathered layer of bedrock. The term comes from the Greek words para, meaning "similar", and *lithic*, meaning "rocky".

to the second stage of magmatic activity of the traps of the Siberian Platform – about 244±5 Ma (see Fig. 3).

5. The structural type anomalies, the nature of which is related to the nature of basites behaviour on the flanks of kimberlite diatrems, were substantiated, which is reasonable to use for their search by geophysical methods [79].

The results obtained about the sequence of formation of Permo-Triassic basites of the Tunguska syneclise will be in demand for solving a wide range of scientific and applied geological issues, such as geodynamic reconstructions of lithospheric plates, clarification of the time of mass extinction of some groups of organisms, petromagnetic correlation and mapping of Siberian traps, mineralogy and prospecting for mineral deposits.

References

1. Lur'e M.L., Polunina L.N., Tuganova E.V. Principles of intrusion dissection in the Late Paleozoic – Early Mesozoic "trap" formation of the Siberian Platform. In: Afanasiev G.D. (ed.). *Petrology and metallogeny of basites.* Moscow: Nauka; 1973, p. 116-126. (In Russ.).

2. Zolotukhin V.V., Vilenskii A.M., Dyuzhikov O.A. *Basalts of the Siberian platform.* Novosibirsk: Nauka; 1986, 245 p. (In Russ.).

3. Parfenov L.M., Kuz'min M.I. *Tectonics, geodynamics and metallogeny of the Sakha Republic (Yakutia).* Moscow: MAIK "Nauka/Interperiodica"; 2001, 517 p. (In Russ.).

4. Polyakov G.V. *Traps of Siberia and the Deccan: similarities and differences.* Novosibirsk: Nauka; 1991, 216 p. (In Russ.).

5. Al'mukhamedov A.I., Medvedev A.Ya., Zolotukhin V.V. Chemical evolution of the permian-triassic basalts of the Siberian Platform in space and time. *Petrologia.* 2004;12(4):339-353. (In Russ.). EDN: OXNOKZ.

6. Masaitis V.L. Permian and Triassic volcanism of Siberia: dynamic reconstruction issues. *Proceedings of the Russian Mineralogical Society.* 1983;112(4):412-425. (In Russ.).

7. Dobretsov N.L., Borisenko A.S., Izokh A.E., Zhmodik S.M. A thermochemical model of Eurasian permo-triassic mantle plumes as a basis for prediction and exploration for Cu-Ni-PGE and rare-metal ore deposits. *Geologiya i geofizika.* 2010;9:1159-1187. (In Russ.). EDN: MVSOEF.

8. Fedorenko V.I., Lightfoot P.C., Naldrett A.J., Czamanske G.K., Hawkesworth C.J., Wooden J.L., et al. Petrogenesis of the floodbasalt sequence at Noril'sk, North Central Siberia. *International Geology Review.* 1996;38(2):99-135.

9. Oleinikov B.V. Geochemical typification of platform basites. In: Koval'skii V.V., Lazebnik K.A., Nikishov K.N. (eds). *Geochemistry and mineralogy of Siberian Platform basites and ultrabasites.* Yakutsk: Yakut Branch of the Siberian Branch of the USSR Academy of Sciences; 1984, p. 4-21. (In Russ.).

10. Tomshin M.D., Kopylova A.G., Tyan O.A. Petrochemical diversity of traps on the eastern periphery of the Tunguska syneclise. *Geologiya i geofizika.* 2005;46(1):72-82. (In Russ.). EDN: MUMSTD.

11. Campbell I.H., Czamanske G.K., Fedorenko VA., Hill R.I., Stepanov V. Synchronism of the Siberian traps and the Permian-Triassic boundary. *Science.* 1992;258(5089):1760-1763. https://doi.org/10.1126/science.258.5089.1760.

12. Wilson J.T. A possible origin of the Hawaiian Islands. *Canadian Journal of Physics.* 1963;41(6):863-870. https://doi.org/10.1139/p63-094.

13. Kuzmin M.I., Yarmolyuk V.V., Kravchinsky V.A. Phanerozoic hot spot traces and paleogeographic reconstructions of the Siberian continent based on interaction with the African large low shear velocity province. *Earth-Science Reviews.* 2010;102(1):29-59. https://doi.org/10.1016/j.earscirev.2010.06.004.

14. Paton M.T., Ivanov A.V., Fiorentini M.L., McNaughton N.J. Mudrovska I., Reznitskii L.Z., et al. Late Permian and Early Triassic magmatic pulses in the Angara-Taseevskaya syncline, South Siberian traps and their possible impact on the environment. *Geologiya i geofizika.* 2010;51(9):1298-1309. (In Russ.). EDN: MVSOGX.

15. Scotese C.R., Langford R.P. Pangea and the paleogeography of the Permian. In: Scholle P.A., Peryt T.M., Ulmer-Scholle D.S. (eds). *The Permian of northern Pangea.* Berlin: Springer-Verlag; 1995, p. 3-19. https://doi.org/10.1007/978-3-642-78593-1_1.

16. Torsvik T.H., Cocks L.R. Triassic. In: Torsvik T.H., Cocks L.R. *Earth history and palaeogeography.* Cambridge: Cambridge University Press; 2016, p. 138-158. https://doi.org/10.1017/9781316225523.012.

17. Remane J., Bassett M.G., Cowie J.W., Gohrbandt K.H., Lane H.R., Michelsen O., et al. Revised guidelines for the establishment of global chronostratigraphic standards by the International Commission on Stratigraphy (ICS). *Episodes.* 1996;19(3):77-81. https://doi.org/10.18814/epiiugs/1996/v19i3/007.

18. Tomshin M.D., Lelyukh M.I., Mishenin S.G., Suntsova S.P., Kopylova A.G., Ubinin S.G. Schematic evolution of trappean magmatism on the eastern side of the Tungus syneclise. *Otechestvennaya Geologiya.* 2001;5:19-24. (In Russ.). EDN: DHDAYX.

19. Kravchinsky V.A., Konstantinov K.M., Courtillot V., Savrasov J.I., Valet J-P., Cherniy S.D., et al. Paleomagnetism of East Siberian traps and kimberlites: two new poles and paleogeographic reconstructions at about 360 and 250 Ma. *Geophysical Journal International.* 2002;148(1):1-33. https://doi.org/10.1046/j.0956-540x.2001.01548.x.

20. Konstantinov K.M., Mishenin S.G, Tomshin M.D., Kornilova V.P., Koval'chuk O.E. Petromagnetic inhomogeneities of the Permian-Triassic traps of the Dalyn-Alakit diamond-bearing region (Western Yakutia). *Lithosphere (Russia).* 2014;2:77-98. (In Russ.). EDN: SGPOVZ.

21. Kirguev A.A., Konstantinov K.M., Kuzina D.M., Makarov A.A., Vasilyeva A.E. Petromagnetic klassification of the basis of the eastern board of the Tungus syneklis. *Journal Geophysics.* 2020;3:45-61. (In Russ.). EDN: FQKOIB.

22. Konstantinov K.M., Kuzina D.M., Khoroshikh M.S. Petrophysical taxa of diamond deposit of Komsomolskaya kimberlite pipe (Yakutsk diamondiferous province). *Earth sciences and subsoil use.* 2024;47(2):190-219. https://doi.org/10.21285/2686-9993-2024-47-2-190-219. EDN: TBAMTC.

23. Vasil'eva A.E., Tomshin M.D., Konstantinov K.M. Trap magmatism of the junction zone of the Tunguska syneclise and the Anabar anteclise. *Nauka i obrazovanie.* 2006;4:40-44. (In Russ.). EDN: KBCYDT.

24. Kutolin V.A. *Problems of basalt petrochemistry and petrology.* Novosibirsk: Nauka; 1972, 208 p. (In Russ.).

25. Kravchinskii A.Ya. *Paleomagnetism and paleogeographic evolution of continents.* Novosibirsk: Nauka; 1979, 264 p. (In Russ.).

26. Khramov A.N., Goncharov G.I., Komissarova R.A., Pisarevskii S.A., Pogarskaya I.A., Rzhevskii Yu.S. *Paleomagnetology.* Leningrad: Nedra; 312 p. (In Russ.).

27. Reichow M.K., Saunders A.D., White R.V., Pringle M.S., Al'mukhamedov A.I., Medvedev A.I., et al. $^{40}Ar/^{39}Ar$ dates from the West Siberian Basin: Siberian flood basalt province doubled. *Science.* 2002;296(5574):1846-1849. https://doi.org/10.1126/science.1071671.

28. Reichow M.K., Pringle M.S., Al'Mukhamedov A.I., Allen M.B., Andreichev V.L., Buslov M.M., et al. The timing and extent of the eruption of the Siberian Traps large igneous province: Implications for the end-Permian environmental crisis. *Earth and Planetary Science Letters.* 2009;277(1-2):9-20. https://doi.org/10.1016/j.epsl.2008.09.030.

29. Renne P.R. Excess ^{40}Ar in biotite and hornblende from the Norilsk 1 intrusion, Siberia: implication for the age of Siberian Traps. *Earth and Planetary Science Letters.* 1995;131(3-4):165-176. https://doi.org/10.1016/0012-821X(95)00015-5.

30. Baksi A.K., Farrar E. $^{40}Ar/^{39}Ar$ dating of the Siberian Traps, USSR: evaluation of the ages of the two major extinction events relative to episodes of flood-basalt volcanism in USS and the Deccan Traps, India. *Geology.* 1991;19(5):461-464. https://doi.org/10.1130/0091-7613(1991)019<0461:ADOTST>2.3.CO;2.

31. Dalrymple G.B., Czamanske G.K., Fedorenko V.A., Simonov O.N., Lanphere M.A., Likhachev A.P. A reconnaissance $^{40}Ar/^{39}Ar$ study of ore-bearing and related rocks, Siberian Russia. *Geochimica et Cosmochimica Acta.* 1995;59(10):2071-2083. https://doi.org/10.1016/0016-7037(95)00127-1.

32. Basu A.R., Poreda R.J., Renne P.R., Teichmann F., Vasiliev Yu.R., Sobolev N.V., et al. High-^{3}He plume origin and temporal-spatial evolution of the Siberian flood basalts. *Science.* 1995;269(5225):822-825. https://doi.org/10.1126/science.269.5225.822.

33. Ivanov A.V., He H., Yang L., Nikolaeva I.V., Palesskii S.V. $^{40}Ar/^{39}Ar$ dating of intrusive magmatism in the Angara-Taseevskaya syncline and its implication for duration of magmatism of the Siberian Traps. *Journal of Asian Earth Sciences.* 2009;35(1):1-12. https://doi.org/10.1016/j.jseaes.2008.11.006.

34. Venkatesan T.R., Kumar A., Gopalan K., Al'mukhamedov A.I. ^{40}Ar-^{39}Ar age of Siberian basaltic volcanism. *Chemical Geology.* 1997;138(3-4):303-310. https://doi.org/10.1016/S0009-2541(97)00006-5.

35. Renne P.R., Basu A.R. Rapid eruption of the Siberian Traps flood basalts at the Permo-Triassic boundary. *Science.* 1991;253(5016):176-179. https://doi.org/10.1126/science.253.5016.176.

36. Mundil R., Ludwig K.R., Metcalfe I., Renne P.R. Age and timing of the Permian mass extinctions: U/Pb dating of closed-system zircons. *Science.* 2004;305(5691):1760-1763. https://doi.org/10.1126/science.1101012.

37. Vernikovsky V.A., Pease V.L., Vernikovskaya A.E., Romanov A.P., Gee D.G., Travin A.V. First report of early Triassic A-type granite and syenite intrusions from Taimyr: Product of the northern Eurasian superplume? *Lithos.* 2003;66(1):23-36. https://doi.org/10.1016/S0024-4937(02)00192-5.

38. Svensen H., Planke S., Polozov A.G., Schmidbauer N., Corfu F., Podladchikov Y.Y., et al. Siberian gas venting and the end-Permian environmental crisis. *Earth and Planetary Science Letters.* 2009;277(3):490-500. https://doi.org/10.1016/j.epsl.2008.11.015.

39. Kuzmichev A.B., Pease V.L. Siberian trap magmatism on the New Siberian Islands: constraints for Arctic Mesozoic plate tectonic reconstructions. *Journal of the Geological Society.* 2007;164(5):959-968. https://doi.org/10.1144/0016-76492006-090.

40. Kamo S.L., Czamanske G.K., Krogh T.E. A minimum U-Pb age for Siberian flood-basalt volcanism. *Geochimica et Cosmochimica Acta.* 1996;60(18):3505-3511. https://doi.org/10.1016/0016-7037(96)00173-1.

41. Kamo S.L., Czamanske G.K., Amelin Yu., Fedorenko V.A., Davis D.W., Trofimov V.R. Rapid eruption of Siberian flood volcanic rocks and evidence for coincidence with the Permian-Triassic boundary and mass extinction at 251 Ma. *Earth and Planetary Science Letters.* 2003;214(1-2):75-91. https://doi.org/10.1016/S0012-821X(03)00347-9.

42. Vladimirov A.G., Kozlov M.S., Shokal'skii S.P., Khalilov V.A., Rudnev S.N., Kruk N.N., et al. Major epochs of intrusive magmatism of Kuznetsk Alatau, Altai, and Kalba (from U-Pb isotope dates). *Geologiya i geofizika.* 2001;42(8):1157-1178. (In Russ.). EDN: MQEUST.

43. Vernikovskaya A.E., Vernikovsky V.A., Matushkin N.Y., Romanova I.V., Berejnaya N.G., Larionov A.N., et al. Middle paleozoic and early mesozoic anorogenic magmatism of the South Yenisei ridge: first geochemical and geochronological data. *Geologiya i geofizika.* 2010;51(5):701-716. (In Russ.). EDN: MKTVLV.

44. Yin H., Zhang K., Tong J., Yang Z., Wu S. The global stratotype section and point (GSSP) of the Permian-Triassic boundary. *Episodes.* 2001;24(2):102-114. https://doi.org/10.18814/epiiugs/2001/v24i2/004.

45. Yin H. On the transitional Bed and the Permian-Triassic boundary in South China. *Newsletter on Stratigraphy.* 1985;15(1):13-27. https://doi.org/10.1127/nos/15/1985/13.

46. Yin H. Reassessment of the index fossils at the Paleozoic-Mesozoic boundary: Palaeoworld, Palaeontology and Stratigraphy Report, Nanjing Institute of Geology and Palaeontology. *Academia Sinica.* 1994;4:153-171.

47. Sheng J., Chen C., Wang Y., Rui L., Liao Z., Bando Y., et al. Permian Triassic boundary in middle and eastern Tethys. *Journal of Faculty of Sciences.* 1984;21(1):133-181.

48. Sheng J., Chen C., Wang Y., Rui L., Liao Z., He J., et al. New advances on the Permian and Triassic boundary of Jiangsu, Zhejiang and Anhui. In: *Stratigraphy and palaeontology of systemic boundaries in China, Permian-Triassic boundary.* Nanjing: Nanjing University Press; 1987, p. 1-22. (In Chinese).

49. Wang C. A conodont-based high-resolution eventostratigraphy and biostratigraphy for the Permian-Triassic boundaries in South China: Palaeoworld, Palaeontology and Stratigraphy. *Academia Sinica.* 1994;4:234-248.

50. Zheng Q.F., Cao C.Q., Zhang M.Y. Sedimentary features of the Permian-Triassic boundary sequence of the Meishan section in Changxing County, Zhejiang Province. *Science China Earth Sciences.* 2013;56:956-969. https://doi.org/10.1007/s11430-013-4602-9.

51. Berman H.M. The Protein Data Bank: a historical perspective. *Acta Crystallographica Section A: Foundations of Crystallography.* 2008;64(1):88-95. https://doi.org/10.1107/S0108767307035623.

52. Mundil R.L., Metcalfe I., Ludwig K.R., Renne P.R., Oberli F., Nicoll R.S. Timing of the Permian-Triassic biotic crisis: implications from new zircon U/Pb age data (and their limitations). *Earth and Planetary Science Letters.* 2001;187 (1-2):131-145.

53. Mundil R., Pálfy J., Renne P.R., Brack P. The Triassic timescale: new constraints and a review of geochronological data. In: Lucas S.G. (ed.). *The Triassic Timescale: Geological Society*. London: Special Publication; 2010, p. 41-60. https://doi.org/10.1144/SP334.3.

54. Claoue-Long J.C., Zhang Z.C., Ma G.G., Du S.H. The age of the Permian-Triassic boundary. *Earth and Planetary Science Letters.* 1991;105(1-3):182-190. https://doi.org/10.1016/0012-821X(91)90129-6.

55. Renne P.R., Zhang Z., Richards M.A., Black M.T., Basu A.R. Synchrony and causal relations between Permian-Triassic boundary crisis and Siberian flood volcanism. *Science.* 1995;269(5229):1413-1416. https://doi.org/10.1126/science.269.5229.1413.

56. Bowring S.A., Erwin D.H., Jin Y.G., Martin M.W., Davidov K., Wang W. U/Pb zircon geochronology and tempo of the end-Permian mass extinction. *Science.* 1998;280(5366):1039-1045. https://doi.org/10.1126/science.280.5366.1039.

57. Metcalfe I., Nicoll R.S., Black L.P., Mundil R., Renne P., Jagodzinski E.A., et al. Isotope geochronology of the Permian-Triassic boundary and mass extinction in South China. In: Hongfu Y., Tong J. (eds). *Pangea and the Paleozoic-Mesozoic transition.* Wuhan: China University of Geosciences Press; 1999, p. 134-137.

58. Zhu Y., Liu Y. Magnetostratigraphy of the Permo-Triassic boundary section at Meishan, Changxing, Zhejiang Province. In: Yin H., Tong J. (eds). *Pangea and the Paleozoic-Mesozoic transition.* Wuhan: China University of Geosciences Press; 1999, p. 79-84.

59. Li H., Wang J. Magnetostratigraphy of Permo-Triassic boundary section of Meishan of Changxing, Zhejiang. *Scientia Sinica: Series B.* 1989;32(11):1401-1408.

60. Heller F., Chen H., Dobson J., Haag M. Permian-Triassic magnetostratigraphy new results from South China. *Physics of the Earth and Planetary Interiors.* 1995;89(3-4):281-295. https://doi.org/10.1016/0031-9201(94)02993-L.

61. Meng X., Hu C., Wang W., Liu H. Magnetostratigraphic study of Meishan Permian-Triassic section, Changxing, Zhejiang Province, China. *Journal of Earth Science.* 2000;11(3):361-365.

62. Min Z., Qin H.-F., He K., Hou Y.-F., Zheng Q.-F., Deng C.-L., et al. Magnetostratigraphy across the end-Permian mass extinction event from the Meishan sections, southeastern China. *Geology.* 2021;49(11):1289-1294. https://doi.org/10.1130/G49072.1.

63. Yuan D.X., Shen S.Z., Henderson C.M., Jun C., Hua Z., Feng H.Z. Revised conodont-based integrated high-resolution timescale for the Changhsingian Stage and end-Permian extinction interval at the Meishan sections, South China. *Lithos.* 2014;204:220-245. https://doi.org/10.1016/j.lithos.2014.03.026.

64. Burgess S.D., Bowring S.A., Shen S.Z. High-precision timeline for Earth's most severe extinction. *Proceedings of the National Academy of Sciences of the United States of America.* 2014;111(9):3316-3321. https://doi.org/10.1073/pnas.1317692111.

65. Shen S.Z., Crowley J.L., Yue W., Bowring S.A., Erwin D.H., Sadler P.M., et al. Calibrating the end-Permian mass extinction. *Science.* 2011;334(6061):1367-1372. https://doi.org/10.1126/science.1213454.

66. Konstantinov K.M., Kuzina D.M., Khoroshikh M.S. Petrophysical taxa of diamond deposit of Komsomolskaya kimberlite pipe (Yakutsk diamondiferous province). *Earth sciences and subsoil use.* 2024;47(2):190-219. https://doi.org/10.21285/2686-9993-2024-47-2-190-219. EDN: TBAMTC.

67. Travin A.V., Yudin D.S., Vladimirov A.G., Khromykh S.V., Volkova N.I., Mekhonoshin A.S., et al. Thermochronology of the Chernorud granulite zone, Ol'khon region, Western Baikal Area. *Geohimiya.* 2009;11:1181-1199. (In Russ.). EDN: KXLBPT.

68. Latyshev A.V., Veselovskiy R.V., Ivanov A.V. Paleomagnetism of the Permian-Triassic intrusions from the Tunguska syncline and the Angara-Taseeva depression, Siberian Traps Large Igneous Province: evidence of contrasting styles of magmatism. *Tectonophysics.* 2018;723:41-55. https://doi.org/10.1016/j.tecto.2017.11.035.

69. Glen J.M.G., Nomade S., Lyons J.J., Metcalfe I., Mundil R., Renne P.R. Magnetostratigraphic correlations of Permian–Triassic marine-to-terrestrial sections from China. *Journal of Asian Earth Sciences.* 2009;36(6):521-540. https://doi.org/10.1016/j.jseaes.2009.03.003.

70. Zakharov Yu.D., Sokarev A.N. Permian–Triassic paleomagnetism of Eurasia. In: *Proceedings of the International Symposium on Shallow Tethys.* 20–23 September 1990, Sendai. Sendai: The Saito Gratitude Foundation; 1991, vol. 3, p. 313-323.

71. Gallet Y., Krystyn L., Besse J., Saidi A., Ricou L.E. New constraints on the Upper Permian and Lower Triassic geomagnetic polarity timescale from the Abadeh section (central Iran). *Journal of Geophysical Research Solid Earth.* 2000;105(B2):2805-2815. https://doi.org/10.1029/1999JB900218.

72. De Kock M.O., Kirschvink J.L. Paleomagnetic constraints on the Permian–Triassic boundary in terrestrial strata of the Karoo Supergroup, South Africa: implications for causes of the end-Permian extinction event. *Gondwana Research.* 2004;7(1):175-183. https://doi.org/10.1016/S1342-937X(05)70316-6.

73. Hounslow M.W., Mork A., Peters C., Weitschat W. Boreal Lower Triassic magnetostratigraphy from Deltadalen, Central Svalbard. *Albertiana.* 1996;17:3-10.

74. Nawrocki J. Permian to Early Triassic magnetostratigraphy from the Central European Basin in Poland: implications on regional and worldwide correlations. *Earth and Planetary Science Letters.* 1997;152(1-4):37-58. https://doi.org/10.1016/S0012-821X(97)00147-7.

75. Szurlies M., Bachmann G.H., Menning M., Nowaczyk N.R., Kaeding K.C. Magnetostratigraphy and high-resolution lithostratigraphy of the Permian–Triassic boundary interval in central Germany. *Earth and Planetary Science Letters.* 2003;212(3-4):263-278. https://doi.org/10.1016/S0012-821X(03)00288-7.

76. Scholger R., Mauritsch H.J., Brandner R. Permian–Triassic boundary magnetostratigraphy from the Southern Alps (Italy). *Earth and Planetary Science Letters.* 2000;176(3-4):495-508. https://doi.org/10.1016/S0012-821X(00)00026-1.

77. Molostovskii A. E., Khramov A. N. Paleomagnetic scale of the Phanerozoic and problems of magnetostratigraphy. In: *Stratigraphy. Reports.* Moscow: Nauka; 1984, vol. 1, p. 16-23. (In Russ.).

78. Kazanskii A.Yu., Kazanskii Yu.P., Saraev S.V., Moskvin V.I. The Permo-Triassic boundary in volcanosedimentary section of the West-Siberian plate according to paleomagnetic data: (from studies of the core from the Tyumenskaya superdeep borehole SD-6). *Geologiya i geofizika.* 2000;41(3):327-339. (In Russ.). EDN: VZVSPQ.

79. Konstantinov K.M., Tomshin M.D., Khoroshikh M.S. Magnetoelastic effect of kimberlite host rocks (Yakutsk diamondiferous province). *Earth sciences and subsoil use*. 2023;46(4):344-363. (In Russ.) https://doi.org/10.21285/2686-9993-2023-46-4-344-363. EDN: GNUPHH.

Список источников

1. Лурье М.Л., Полунина Л.Н., Туганова Е.В. Принципы расчленения интрузивов позднепалеозойско-раннемезозойской «трапповой» формации Сибирской платформы // Петрология и металлогения базитов / под ред. Г.Д. Афанасьева. М.: Наука, 1973. С. 116–126.

2. Золотухин В.В., Виленский А.М., Дюжиков О.А. Базальты Сибирской платформы. Новосибирск: Наука, 1986, 245 с.

3. Л.М. Парфенов, М.И. Кузьмин. Тектоника, геодинамика и металлогения территории Республики Саха (Якутия). М.: МАИК «Наука/Интерпериодика», 2001. 517 с.

4. Поляков Г.П. Траппы Сибири и Декана: черты сходства и различия. Новосибирск: Наука, 1991. 216 с.

5. Альмухамедов А.И., Медведев А.Я., Золотухин В.В. Вещественная эволюция пермотриасовых базальтов Сибирской платформы во времени и пространстве // Петрология. 2004. Т. 12. № 4. С. 339–353. EDN: OXNOKZ.

6. Масайтис В.Л. Пермский и триасовый вулканизм Сибири: проблемы динамических реконструкций // Записки Всесоюзного минералогического общества. 1983. Т. 112. № 4. С. 412–425.

7. Добрецов Н.Л., Борисенко А.С., Изох А.Э., Жмодик С.М. Термохимическая модель пермотриасовых мантийных плюмов Евразии как основа для выявления закономерностей формирования и прогноза медно-никелевых, благородно- и редкометальных месторождений // Геология и геофизика. 2010. № 9. С. 1159–1187. EDN: MVSOEF.

8. Fedorenko V.I., Lightfoot P.C., Naldrett A.J., Czamanske G.K., Hawkesworth C.J., Wooden J.L., et al. Petrogenesis of the floodbasalt sequence at Noril'sk, North Central Siberia // International Geology Review. 1996. Vol. 38. Iss. 2. P. 99–135.

9. Олейников Б.В. Геохимическая типизация платформенных базитов // Геохимия и минералогия базитов и ультрабазитов Сибирской платформы / под ред. В.В. Ковальского, К.А. Лазебник, К.Н. Никишова. Якутск: Изд-во ЯФ СО АН СССР, 1984. С. 4–21.

10. Томшин М.Д., Копылова А.Г., Тян О.А. Петрохимическое разнообразие траппов восточной периферии Тунгусской синеклизы // Геология и геофизика. 2005. Т. 46. № 1. С. 72–82. EDN: MUMSTD.

11. Campbell I.H., Czamanske G.K., Fedorenko VA., Hill R.I., Stepanov V. Synchronism of the Siberian traps and the Permian-Triassic boundary // Science. 1992. Vol. 258. Iss. 5089. P. 1760–1763. https://doi.org/10.1126/science.258.5089.1760.

12. Wilson J.T. A possible origin of the Hawaiian Islands // Canadian Journal of Physics. 1963. Vol. 41. Iss. 6. P. 863–870. https://doi.org/10.1139/p63-094.

13. Kuzmin M.I., Yarmolyuk V.V., Kravchinsky V.A. Phanerozoic hot spot traces and paleogeographic reconstructions of the Siberian continent based on interaction with the African large low shear velocity province // Earth-Science Reviews. 2010. Vol. 102. Iss. 1. P. 29–59. https://doi.org/10.1016/j.earscirev.2010.06.004.

14. Патон М.Т., Иванов А.В., Фиорентини М.Л., Мак-Наугтон Н.Ж., Мудровская И., Резницкий Л.З. [и др.]. Позднепермские и раннетриасовые магматические импульсы в Ангаро-Тасеевской синклинали, Южно-Сибирские траппы и их возможное влияние на окружающую среду // Геология и геофизика. 2010. Т. 51. № 9. С. 1298–1309. EDN: MVSOGX.

15. Scotese C.R., Langford R.P. Pangea and the paleogeography of the Permian // The Permian of northern Pangea / eds P.A. Scholle, T.M. Peryt, D.S. Ulmer-Scholle. Berlin: Springer-Verlag, 1995. P. 3–19. https://doi.org/10.1007/978-3-642-78593-1_1.

16. Torsvik T.H., Cocks L.R. Triassic // Earth history and palaeogeography / T.H. Torsvik, L.R. Cocks. Cambridge: Cambridge University Press, 2016. P. 138–158. https://doi.org/10.1017/9781316225523.012.

17. Remane J., Bassett M.G., Cowie J.W., Gohrbandt K.H., Lane H.R., Michelsen O., et al. Revised guidelines for the establishment of global chronostratigraphic standards by the International Commission on Stratigraphy (ICS) // Episodes. 1996. Vol. 19. Iss. 3. P. 77–81. https://doi.org/10.18814/epiiugs/1996/v19i3/007.

18. Томшин М.Д., Лелюх М.И., Мишенин С.Г., Сунцова С.П., Копылова А.Г., Убинин С.Г. Схема развития траппового магматизма восточного борта Тунгусской синеклизы // Отечественная геология. 2001. № 5. С. 19–24. EDN: DHDAYX.

19. Kravchinsky V.A., Konstantinov K.M., Courtillot V., Savrasov J.I., Valet J-P., Cherniy S.D., et al. Paleomagnetism of East Siberian traps and kimberlites: two new poles and paleogeographic reconstructions at about 360 and 250 Ma // Geophysical Journal International. 2002. Vol. 148. Iss. 1. P. 1–33. https://doi.org/10.1046/j.0956-540x.2001.01548.x.

20. Константинов К.М., Мишенин С.Г, Томшин М.Д., Корнилова В.П., Ковальчук О.Е. Петромагнитные неоднородности пермотриасовых траппов Далдыно-Алакитского алмазоносного района (Западная Якутия) // Литосфера. 2014. № 2. С. 77–98. EDN: SGPOVZ.

21. Киргуев А.А., Константинов К.М., Кузина Д.М., Макаров А.А., Васильева А.Е. Петромагнитная классификация базитов восточного борта Тунгуской синеклизы // Геофизика. 2020. № 3. С. 45–61. EDN: FQKOIB.

22. Konstantinov K.M., Kuzina D.M., Khoroshikh M.S. Petrophysical taxa of diamond deposit of Komsomolskaya kimberlite pipe (Yakutsk diamondiferous province) // Науки о Земле и недропользование. 2024. Т. 47. № 2. С. 190–219. https://doi.org/10.21285/2686-9993-2024-47-2-190-219. EDN: TBAMTC.

23. Васильева А.Е., Томшин М.Д., Константинов К.М. Трапповый магматизм зоны сочленения Тунгусской синеклизы и Анабарской антеклизы // Наука и образование. 2006. № 4. С. 40–44. EDN: KBCYDT.

24. Кутолин В.А. Проблемы петрохимии и петрологии базальтов. Новосибирск: Наука, 1972. 208 с.

25. Кравчинский А.Я. Палеомагнетизм и палеогеографическая эволюция континентов. Новосибирск: Наука, 1979. 264 с.

26. Храмов А.Н., Гончаров Г.И., Комиссарова Р.А., Писаревский С.А., Погарская И.А., Ржевский Ю.С. [и др.]. Палеомагнитология. Л.: Недра, 1982. 312 с.

27. Reichow M.K., Saunders A.D., White R.V., Pringle M.S., Al'mukhamedov A.I., Medvedev A.I., et al. $^{40}Ar/^{39}Ar$ dates from the West Siberian Basin: Siberian flood basalt province doubled // Science. 2002. Vol. 296. Iss. 5574. P. 1846–1849. https://doi.org/10.1126/science.1071671.

28. Reichow M.K., Pringle M.S., Al'Mukhamedov A.I., Allen M.B., Andreichev V.L., Buslov M.M., et al. The timing and extent of the eruption of the Siberian Traps large igneous province: Implications for the end-Permian environmental crisis // Earth and Planetary Science Letters. 2009. Vol. 277. Iss. 1–2. P. 9–20. https://doi.org/10.1016/j.epsl.2008.09.030.

29. Renne P.R. Excess ^{40}Ar in biotite and hornblende from the Norilsk 1 intrusion, Siberia: implication for the age of Siberian Traps // Earth and Planetary Science Letters. 1995. Vol. 131. Iss. 3–4. P. 165–176. https://doi.org/10.1016/0012-821X(95)00015-5.

30. Baksi A.K., Farrar E. $^{40}Ar/^{39}Ar$ dating of the Siberian Traps, USSR: evaluation of the ages of the two major extinction events relative to episodes of flood-basalt volcanism in USS and the Deccan Traps, India // Geology. 1991. Vol. 19. Iss. 5. P. 461–464. https://doi.org/10.1130/0091-7613(1991)019<0461:ADOTST>2.3.CO;2.

31. Dalrymple G.B., Czamanske G.K., Fedorenko V.A., Simonov O.N., Lanphere M.A., Likhachev A.P. A reconnaissance $^{40}Ar/^{39}Ar$ study of ore-bearing and related rocks, Siberian Russia // Geochimica et Cosmochimica Acta. 1995. Vol. 59. Iss. 10. P. 2071–2083. https://doi.org/10.1016/0016-7037(95)00127-1.

32. Basu A.R., Poreda R.J., Renne P.R., Teichmann F., Vasiliev Yu.R., Sobolev N.V., et al. High-^{3}He plume origin and temporal-spatial evolution of the Siberian flood basalts // Science. 1995. Vol. 269. Iss. 5225. P. 822–825. https://doi.org/10.1126/science.269.5225.822.

33. Ivanov A.V., He H., Yang L., Nikolaeva I.V., Palesskii S.V. $^{40}Ar/^{39}Ar$ dating of intrusive magmatism in the Angara-Taseevskaya syncline and its implication for duration of magmatism of the Siberian Traps // Journal of Asian Earth Sciences. 2009. Vol. 35. Iss. 1. P. 1–12. https://doi.org/10.1016/j.jseaes.2008.11.006.

34. Venkatesan T.R., Kumar A., Gopalan K., Al'mukhamedov A.I. ^{40}Ar-^{39}Ar age of Siberian basaltic volcanism // Chemical Geology. 1997. Vol. 138. Iss. 3–4. P. 303–310. https://doi.org/10.1016/S0009-2541(97)00006-5.

35. Renne P.R., Basu A.R. Rapid eruption of the Siberian Traps flood basalts at the Permo-Triassic boundary // Science. 1991. Vol. 253. Iss. 5016. P. 176–179. https://doi.org/10.1126/science.253.5016.176.

36. Mundil R., Ludwig K.R., Metcalfe I., Renne P.R. Age and timing of the Permian mass extinctions: U/Pb dating of closed-system zircons // Science. 2004. Vol. 305. Iss. 5691. P. 1760–1763. https://doi.org/10.1126/science.1101012.

37. Vernikovsky V.A., Pease V.L., Vernikovskaya A.E., Romanov A.P., Gee D.G., Travin A.V. First report of early Triassic A-type granite and syenite intrusions from Taimyr: Product of the northern Eurasian superplume? // Lithos. 2003. Vol. 66. Iss. 1. P. 23–36. https://doi.org/10.1016/S0024-4937(02)00192-5.

38. Svensen H., Planke S., Polozov A.G., Schmidbauer N., Corfu F., Podladchikov Y.Y., et al. Siberian gas venting and the end-Permian environmental crisis // Earth and Planetary Science Letters. 2009. Vol. 277. Iss. 3. P. 490–500. https://doi.org/10.1016/j.epsl.2008.11.015.

39. Kuzmichev A.B., Pease V.L. Siberian trap magmatism on the New Siberian Islands: constraints for Arctic Mesozoic plate tectonic reconstructions // Journal of the Geological Society. 2007. Vol. 164. Iss. 5. P. 959–968. https://doi.org/10.1144/0016-76492006-090.

40. Kamo S.L., Czamanske G.K., Krogh T.E. A minimum U-Pb age for Siberian flood-basalt volcanism // Geochimica et Cosmochimica Acta. 1996. Vol. 60. Iss. 18. P. 3505–3511. https://doi.org/10.1016/0016-7037(96)00173-1.

41. Kamo S.L., Czamanske G.K., Amelin Yu., Fedorenko V.A., Davis D.W., Trofimov V.R. Rapid eruption of Siberian flood volcanic rocks and evidence for coincidence with the Permian-Triassic boundary and mass extinction at 251 Ma // Earth and Planetary Science Letters. 2003. Vol. 214. Iss. 1–2. P. 75–91. https://doi.org/10.1016/S0012-821X(03)00347-9.

42. Владимиров А.Г., Козлов М.С., Шокальский С.П., Халилов В.А., Руднев С.Н., Крук Н.Н. [и др.]. Основные возрастные рубежи интрузивного магматизма Кузнецкого Алатау и Калбы (по данным U-Pb изотопного датирования) // Геология и геофизика. 2001. Т. 42. № 8. С. 1157–1178. EDN: MQEUST.

43. Верниковская А.Е., Верниковский В.А., Матушкин Н.Ю., Романова И.В., Бережная Н.Г., Ларионов А.Н. [и др.]. Среднепалеозойский и раннемезозойский анорогенный магматизм Южно-Енисейского кряжа: первые геохимические и геохронологические данные // Геология и геофизика. 2010. Т. 51. № 5. С. 701–716. EDN: MKTVLV.

44. Yin H., Zhang K., Tong J., Yang Z., Wu S. The global stratotype section and point (GSSP) of the Permian-Triassic boundary // Episodes. 2001. Vol. 24. Iss. 2. P. 102–114. https://doi.org/10.18814/epiiugs/2001/v24i2/004.

45. Yin H. On the transitional Bed and the Permian-Triassic boundary in South China // Newsletter on Stratigraphy. 1985. Vol. 15. Iss. 1. P. 13–27. https://doi.org/10.1127/nos/15/1985/13.

46. Yin H. Reassessment of the index fossils at the Paleozoic-Mesozoic boundary: Palaeoworld, Palaeontology and Stratigraphy Report, Nanjing Instiftute of eology and Palaeontology // Academia Sinica. 1994. Iss. 4. P. 153–171.

47. Sheng J., Chen C., Wang Y., Rui L., Liao Z., Bando Y., et al. Permian Triassic boundary in middle and eastern Tethys // Journal of Faculty of Sciences. 1984. Vol. 21. Iss. 1. P.133–181.

48. Sheng J., Chen C., Wang Y., Rui L., Liao Z., He J., et al. New advances on the Permian and Triassic boundary of Jiangsu, Zhejiang and Anhui // Stratigraphy and palaeontology of systemic boundaries in China, Permian-Triassic boundary. Nanjing: Nanjing University Press, 1987. P. 1–22.

49. Wang C. A conodont-based high-resolution eventostratigraphy and biostratigraphy for the Permian-Triassic boundaries in South China: Palaeoworld, Palaeontology and Stratigraphy // Academia Sinica. 1994. Iss. 4. P. 234–248.

50. Zheng Q.F., Cao C.Q., Zhang M.Y. Sedimentary features of the Permian-Triassic boundary sequence of the Meishan section in Changxing County, Zhejiang Province // Science China Earth Sciences. 2013. Vol. 56. P. 956–969. https://doi.org/10.1007/s11430-013-4602-9.

51. Berman H.M. The Protein Data Bank: a historical perspective // Acta Crystallographica Section A: Foundations of Crystallography. 2008. Vol. 64. Iss. 1. P. 88–95. https://doi.org/10.1107/S0108767307035623.

52. Mundil R.L., Metcalfe I., Ludwig K.R., Renne P.R., Oberli F., Nicoll R.S. Timing of the Permian-Triassic biotic crisis: implicationsfrom new zircon U/Pb age data (and their limitations) // Earth and Planetary Science Letters. 2001. Vol. 187. Iss. 1–2. P. 131–145.

53. Mundil R., Pálfy J., Renne P.R., Brack P. The Triassic timescale: new constraints and a review of geochronological data // The Triassic Timescale: Geological Society / ed. S.G. Lucas. London: Special Publication, 2010. P. 41–60. https://doi.org/10.1144/SP334.3.

54. Claoue-Long J.C., Zhang Z.C., Ma G.G., Du S.H. The age of the Permian-Triassic boundary // Earth and Planetary Science Letters. 1991. Vol. 105. Iss. 1–3. P. 182–190. https://doi.org/10.1016/0012-821X(91)90129-6.

55. Renne P.R., Zhang Z., Richards M.A., Black M.T., Basu A.R. Synchrony and causal relations between Permian-Triassic boundary crisis and Siberian flood volcanism // Science. 1995. Vol. 269. Iss. 5229. P. 1413–1416. https://doi.org/10.1126/science.269.5229.1413.

56. Bowring S.A., Erwin D.H., Jin Y.G., Martin M.W., Davidov K., Wang W. U/Pb zircon geochronology and tempo of the end-Permian mass extinction // Science. 1998. Vol. 280. Iss. 5366. P. 1039–1045. https://doi.org/10.1126/science.280.5366.1039.

57. Metcalfe I., Nicoll R.S., Black L.P., Mundil R., Renne P., Jagodzinski E.A., et al. Isotope geochronology of the Permian-Triassic boundary and mass extinction in South China // Pangea and the Paleozoic-Mesozoic transition / eds Y. Hongfu, J. Tong. Wuhan: China University of Geosciences Press, 1999. P. 134–137.

58. Zhu Y., Liu Y. Magnetostratigraphy of the Permo-Triassic boundary section at Meishan, Changxing, Zhejiang Province // Pangea and the Paleozoic-Mesozoic transition / eds H. Yin, J. Tong. Wuhan: China University of Geosciences Press, 1999. P. 79–84.

59. Li H., Wang J. Magnetostratigraphy of Permo-Triassic boundary section of Meishan of Changxing, Zhejiang // Scientia Sinica: Series B. 1989. Vol. 32. Iss. 11. P. 1401–1408.

60. Heller F., Chen H., Dobson J., Haag M. Permian-Triassic magnetostratigraphy new results from South China // Physics of the Earth and Planetary Interiors. 1995. Vol. 89. Iss. 3–4. P. 281–295. https://doi.org/10.1016/0031-9201(94)02993-L.

61. Meng X., Hu C., Wang W., Liu H. Magnetostratigraphic study of Meishan Permian-Triassic section, Changxing, Zhejiang Province, China // Journal of Earth Science. 2000. Vol. 11. Iss. 3. P. 361–365.

62. Min Z., Qin H.-F., He K., Hou Y.-F., Zheng Q.-F., Deng C.-L., et al. Magnetostratigraphy across the end-Permian mass extinction event from the Meishan sections, southeastern China // Geology. 2021. Vol. 49. Iss. 11. P. 1289–1294. https://doi.org/10.1130/G49072.1.

63. Yuan D.X., Shen S.Z., Henderson C.M., Jun C., Hua Z., Feng H.Z. Revised conodont-based integrated high-resolution timescale for the Changhsingian Stage and end-Permian extinction interval at the Meishan sections, South China // Lithos. 2014. Vol. 204. P. 220–245. https://doi.org/10.1016/j.lithos.2014.03.026.

64. Burgess S.D., Bowring S.A., Shen S.Z. High-precision timeline for Earth's most severe extinction // Proceedings of the National Academy of Sciences of the United States of America. 2014. Vol. 111. Iss. 9. P. 3316–3321. https://doi.org/10.1073/pnas.1317692111.

65. Shen S.Z., Crowley J.L., Yue W., Bowring S.A., Erwin D.H., Sadler P.M., et al. Calibrating the end-Permian mass extinction // Science. 2011. Vol. 334. Iss. 6061. P. 1367–1372. https://doi.org/10.1126/science.1213454.

66. Konstantinov K.M., Kuzina D.M., Khoroshikh M.S. Petrophysical taxa of diamond deposit of Komsomolskaya kimberlite pipe (Yakutsk diamondiferous province) // Науки о Земле и недропользование. 2024. Т. 47. № 2. С. 190–219. https://doi.org/10.21285/2686-9993-2024-47-2-190-219. EDN: TBAMTC.

67. Травин А.В., Юдин Д.С., Владимиров А.Г., Хромых С.В., Волкова Н.И., Мехоношин А.С. [и др.]. Термохронология Чернорудской гранулитовой зоны (Ольхонский регион, Западное Прибайкалье) // Геохимия. 2009. № 11. С. 1181–1199. EDN: KXLBPT.

68. Latyshev A.V., Veselovskiy R.V., Ivanov A.V. Paleomagnetism of the Permian-Triassic intrusions from the Tunguska syncline and the Angara-Taseeva depression, Siberian Traps Large Igneous Province: evidence of contrasting styles of magmatism // Tectonophysics. 2018. Vol. 723. P. 41–55. https://doi.org/10.1016/j.tecto.2017.11.035.

69. Glen J.M.G., Nomade S., Lyons J.J., Metcalfe I., Mundil R., Renne P.R. Magnetostratigraphic correlations of Permian–Triassic marine-to-terrestrial sections from China // Journal of Asian Earth Sciences. 2009. Vol. 36. Iss. 6. P. 521–540. https://doi.org/10.1016/j.jseaes.2009.03.003.

70. Zakharov Yu.D., Sokarev A.N. Permian–Triassic paleomagnetism of Eurasia // Proceedings of the International Symposium on Shallow Tethys (Sendai, 20–23 September 1990). Sendai: The Saito Gratitude Foundation, 1991. Vol. 3. P. 313–323.

71. Gallet Y., Krystyn L., Besse J., Saidi A., Ricou L.E. New constraints on the Upper Permian and Lower Triassic geomagnetic polarity timescale from the Abadeh section (central Iran) // Journal of Geophysical Research Solid Earth. 2000. Vol. 105. Iss. B2. P. 2805–2815. https://doi.org/10.1029/1999JB900218.

72. De Kock M.O., Kirschvink J.L. Paleomagnetic constraints on the Permian–Triassic boundary in terrestrial strata of the Karoo Supergroup, South Africa: implications for causes of the end-Permian extinction event // Gondwana Research. 2004. Vol. 7. Iss. 1. P. 175–183. https://doi.org/10.1016/S1342-937X(05)70316-6.

73. Hounslow M.W., Mork A., Peters C., Weitschat W. Boreal Lower Triassic magnetostratigraphy from Deltadalen, Central Svalbard // Albertiana. 1996. Vol. 17. P. 3–10.

74. Nawrocki J. Permian to Early Triassic magnetostratigraphy from the Central European Basin in Poland: implications on regional and worldwide correlations // Earth and Planetary Science Letters. 1997. Vol. 152. Iss. 1–4. P. 37–58. https://doi.org/10.1016/S0012-821X(97)00147-7.

75. Szurlies M., Bachmann G.H., Menning M., Nowaczyk N.R., Kaeding K.C. Magnetostratigraphy and high-resolution lithostratigraphy of the Permian–Triassic boundary interval in central Germany // Earth and Planetary Science Letters. 2003. Vol. 212. Iss. 3–4. P. 263–278. https://doi.org/10.1016/S0012-821X(03)00288-7.

76. Scholger R., Mauritsch H.J., Brandner R. Permian–Triassic boundary magnetostratigraphy from the Southern Alps (Italy) // Earth and Planetary Science Letters. 2000. Vol. 176. Iss. 3–4. P. 495–508. https://doi.org/10.1016/S0012-821X(00)00026-1.

77. Молостовский А.Э., Храмов А.Н. Палеомагнитная шкала фанерозоя и проблемы магнитостратиграфии // Стратиграфия. Доклады. М.: Наука, 1984. Т. 1. С. 16–23.

78. Казанский А.Ю., Казанский Ю.П., Сараев С.В., Москвин В.И. Граница перми и триаса в вулканогенно-осадочном разрезе Западно-Сибирской плиты по палеомагнитным данным (по материалам изучения керна Тюменской сверхглубокой скважины SD-6) // Геология и геофизика. 2000. Т. 41. С. 327–339. EDN: VZVSPQ.

79. Константинов К.М., Томшин М.Д., Хороших М.С. Магнитоупругий эффект кимберлитовмещающих пород (Якутская алмазоносная провинция) // Науки о Земле и недропользование. 2023. Т. 46. № 4. С. 344–363. https://doi.org/10.21285/2686-9993-2023-46-4-344-363. EDN: GNUPHH.

Information about the authors / Информация об авторах

Konstantin M. Konstantinov,
Dr. Sci. (Geol. & Mineral.),
Head of the Geophysics Department,
Siberian School of Geosciences,
Irkutsk National Research Technical University,
Irkutsk, Russia,
✉ konstantinovkm@ex.istu.edu
https://orcid.org/0000-0002-1196-8776
Константинов Константин Михайлович,
доктор геолого-минералогических наук,
руководитель департамента геофизики,
институт «Сибирская школа геонаук»,
Иркутский национальный исследовательский технический университет,
г. Иркутск, Россия,
✉ konstantinovkm@ex.istu.edu
https://orcid.org/0000-0002-1196-8776

Mikhail D. Tomshin,
Cand. Sci. (Geol. & Mineral.),
Senior Researcher,
Head of the Geological Museum Laboratory,
Diamond and Precious Metal Geology Institute, Siberian Branch
of the Russian Academy of Sciences,
Yakutsk, Russia,
tmd@diamond.ysn.ru
https://orcid.org/0000-0001-5865-7521
Томшин Михаил Дмитриевич,
кандидат геолого-минералогических наук,
старший научный сотрудник,
заведующий лабораторией «Геологический музей»,
Институт геологии алмаза и благородных металлов СО РАН,
г. Якутск, Россия,
tmd@diamond.ysn.ru
https://orcid.org/0000-0001-5865-7521

Innokenty K. Konstantinov,
Research Engineer,
Ore Geology Department,
Siberian School of Geosciences,
Irkutsk National Research Technical University,
Irkutsk, Russia,
geologiaforever@mail.ru
https://orcid.org/0009-0009-5013-6241
Константинов Иннокентий Константинович,
инженер-исследователь,
департамент рудной геологии,
институт «Сибирская школа геонаук»,
Иркутский национальный исследовательский технический университет,
г. Иркутск, Россия,
geologiaforever@mail.ru
https://orcid.org/0009-0009-5013-6241

Anatoly N. Popov,
Student,
Siberian School of Geosciences,
Irkutsk National Research Technical University,
Irkutsk, Russia,
anatoliy_popov_04@mail.ru
https://orcid.org/0009-0008-7764-8100
Попов Анатолий Николаевич,
студент,
институт «Сибирская школа геонаук»,
Иркутский национальный исследовательский технический университет,
г. Иркутск, Россия,
anatoliy_popov_04@mail.ru
https://orcid.org/0009-0008-7764-8100

Veniamin E. Pozdniakov,
Student,
Institute of High Technologies,
Laboratory Research Assistant at the Chemical Analytical Laboratory,
Siberian School of Geosciences,
Irkutsk National Research Technical University,
Irkutsk, Russia,
venya081004@gmail.com
https://orcid.org/0009-0002-6006-9416

Поздняков Вениамин Егорович,
студент,
Институт высоких технологий,
лаборант-исследователь химико-аналитической лаборатории,
институт «Сибирская школа геонаук»,
Иркутский национальный исследовательский технический университет,
г. Иркутск, Россия,
venya081004@gmail.com
https://orcid.org/0009-0002-6006-9416

Shen Yi,
Student,
School of Geography,
Nanjing Normal University,
Nanjing, China,
15962597891@163.com
https://orcid.org/0009-0005-1961-5157
И Шэнь,
студент,
Школа географии,
Нанкинский педагогический университет,
г. Нанкин, Китай,
15962597891@163,com
https://orcid.org/0009-0005-1961-5157

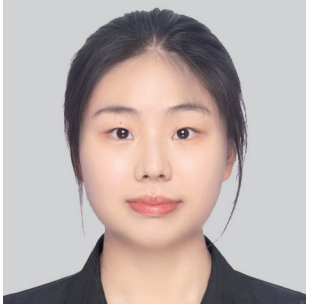

Zitong Zhou,
Student,
Institute of Foreign Languages,
Nanjing University,
Nanjing, China,
2496383208@qq.com
https://orcid.org/0009-0000-7524-2723
Чжоу Цзытун,
студент,
Институт иностранных языков,
Нанкинский университет,
г. Нанкин, Китай,
2496383208@qq,com
https://orcid.org/0009-0000-7524-2723

Contribution of the authors / Вклад авторов

Konstantin M. Konstantinov – conceptualization, investigation, writing – original draft, writing – editing.
Mikhail D. Tomshin – investigation, writing – original draft, writing – editing.
Innokenty K. Konstantinov – investigation, formal analysis.
Anatoly N. Popov – investigation, visualization.
Veniamin E. Pozdniakov – investigation, visualization.
Shen Yi – investigation.
Zhou Zitong – investigation.
К.М. Константинов – разработка концепции, проведение исследования, написание черновика рукописи, редактирование рукописи.
М.Д. Томшин – проведение исследования, написание черновика рукописи, редактирование рукописи.
И.К. Константинов – проведение исследования, формальный анализ.
А.П. Попов – проведение исследования, визуализация.
В.Е. Поздняков – проведение исследования, визуализация.
И Шень – проведение исследования.
Ц. Чжоу – проведение исследования.

Conflict of interests / Конфликт интересов

The authors declare no conflicts of interests.
Авторы заявляют об отсутствии конфликта интересов.

The final manuscript has been read and approved by all the co-authors.
Все авторы прочитали и одобрили окончательный вариант рукописи.

Information about the article / Информация о статье

The article was submitted 17.02.2025; approved after reviewing 25.02.2025; accepted for publication 03.03.2025.
Статья поступила в редакцию 17.02.2025; одобрена после рецензирования 25.02.2025; принята к публикации 03.03.2025.